

# Molecular-Spintronics: the art of driving spin through molecules

S. Sanvito\* and A. R. Rocha  
School of Physics, Trinity College, Dublin 2, IRELAND  
(Dated: 29th October 2018)

*Spintronics* is the ability of injecting, manipulating and detecting electron spins into solid state systems. Molecular-electronics investigates the possibility of making electronic devices using organic molecules. Traditionally these two burgeoning areas have lived separate lives, but recently a growing number of experiments have indicated a possible pathway towards their integration. This is the playground for *molecular-spintronics*, where spin-polarized currents are carried through molecules, and in turn they can affect the state of the molecule. We review the most recent advances in molecular-spintronics. In particular we discuss how a fully quantitative theory for spin-transport in nanostructures can offer fundamental insights into the main factors affecting spin-transport at the molecular level, and can help in designing novel concept devices.

PACS numbers:

## Contents

<b>I. Introduction</b>	1
<b>II. Spin-Electronics</b>	2
A. Transition metals and spin valves	2
B. Spin valves	3
C. Spin polarization of a device	4
<b>III. Molecular-Electronics</b>	4
A. Electrons transport through molecules	4
B. The bonding with the contacts	5
C. Why spins and molecules?	6
<b>IV. Quantitative Transport Theory</b>	7
A. Simple Model	7
B. <i>Ab initio</i> methods	8
<b>V. Molecular Spin-valves</b>	9
A. Metallic and tunneling junctions	9
B. Carbon Nanotubes	13
C. Long molecules and phonons	14
<b>VI. More exotic phenomena</b>	15
A. Molecular Magnets	15
B. $d^0$ ferromagnetism and magnetic proximity	16
<b>VII. Conclusions</b>	17
<b>Acknowledgement</b>	17
<b>References</b>	17

## I. INTRODUCTION

Very few scientific discoveries have moved from an academic laboratory to industrial mass production as quickly as the giant magnetoresistance effect (GMR)<sup>1,2</sup>, now exploited in any read-head for standard hard drives. GMR is the change of the electrical resistance of a magnetic device when an external magnetic field is applied

and it is essentially associated to a change in the magnetic state of the device itself. The revolutionary scientific message revealed by the GMR effect is that the electron spin, as well as the electronic charge, can be used in electronic applications. This somehow has set a new paradigm.

More recently, the electron spin has made its appearance in semiconductor physics. This new field, usually called spin-electronics or spintronics<sup>3,4,5</sup> has the potential of bringing memory and logic functionalities on the same chip. The electron spin is the ultimate logic bit. In semiconductors spin preserves coherence over extremely long times<sup>6</sup> and distances<sup>7</sup>, thus it offers the tantalizing prospect of being used for quantum logic<sup>8</sup>. Moreover all electronic ways of manipulating the spin direction have been proposed<sup>9</sup>. These are based on the spin-orbit interaction<sup>10</sup>, which interestingly plays a ubiquitous rôle in semiconductor spintronics.

On the one hand spin-orbit allows us to manipulate the electron spins by electric only means. It is an intrinsic property of the electronic structure, and therefore it can be engineered by appropriate heterojunction fabrication and manipulated by stress or with an external electric field. Importantly it can be controlled, at least in principle, at an extremely local level. The spin Hall<sup>11</sup> effect, a solid state version of the Stern-Gerlach experiment utilizing spin-orbit interaction instead of a magnetic field gradient, is a good example of all-electrical spin manipulation. On the other hand spin-orbit is the main source of spin-dephasing through the Dyakonov-Perel mechanism<sup>12</sup>, i.e. in semiconductors it is the main interaction responsible for reducing spin coherence.

Ultimately spin looks like an attractive degree of freedom to be used in logic because the energy scale relevant for its typical dynamics is order of magnitudes smaller than that involved in manipulating the electron charge in standard transistors. This can translate in devices exhibiting ultra-low power consumption and high speed. Moreover the sole existence of magnetic materials with high Curie temperature suggests the possibility of powerless non-volatility.

At the same time and almost in parallel there has been a growing interest in making electronic devices using organic molecules. This field, which takes the suggestive name of molecular-electronics<sup>13</sup>, aims at replacing standard semiconductors with organic materials. These have the advantages to be manufactured with low-temperature low-cost chemical methods, instead of expensive high-temperature solid-state growth (e.g. molecular beam epitaxy) and patterning (lithography) techniques. In addition the endless possibilities of chemical synthesis and end-groups engineering give good expectation for new concept devices. Negative differential resistance<sup>14</sup> and rectification<sup>15</sup> have been already proved at the molecular level and prototypes of molecular transistors<sup>17</sup>, memories<sup>16</sup> and logic gates<sup>18,19</sup>, have all been demonstrated.

It is only until recently that spin has entered the realm of molecular electronics. The driving idea behind the first pioneering experiment of Tsukagoshi and coworkers<sup>20</sup>, who injected spin polarized electrons into carbon nanotubes, is that spin-orbit interaction is very weak in carbon-based materials. This fact, in addition to the rather weak hyperfine interaction, suggests extremely long spin relaxation times, and therefore the possibility of coherent spin propagation over large distances. A rather conservative estimate of the spin diffusion length from the Tsukagoshi's experiment indicated 130 nm as a lower bound of the spin-diffusion in carbon nanotubes. These findings have stimulated a growing activity in the area and several experiments dealing with molecular tunneling junctions<sup>21</sup>, spin-transport through polymers<sup>22,23</sup> and optical pump/probe experiments through molecular bridges<sup>24</sup> have recently appeared.

The molecular world has all the ingredients that spin-electronics needs. The conductivity of polymers can be changed by more than ten order of magnitudes<sup>25</sup> and elementary molecules can be designed with the desired electronic structure. Molecules can be anchored to metals in numerous ways and the bonding angle can be further engineered by the coverage density. The spin-relaxation times can be extremely long and furthermore both paramagnetic and ferromagnetic molecules<sup>26</sup> are available.

Theory and modeling is a powerful engine for the development of this new area. At present accurate quantitative algorithms for evaluating the  $I$ - $V$  characteristics of molecular devices are available<sup>27,28,29,30,31,32,33</sup>, and they are revolutionarizing the world of nanoscale device simulators, as density functional theory (DFT)<sup>34</sup> did for electronic structure methods in the sixties. Some of these algorithms are spin polarized<sup>27,28,29,32</sup>, and therefore readily applicable to spin-transport phenomena. Certainly such calculations are not easy. For instance the degree of accuracy needed for the description of the underling electronic structure may go beyond what is standard in solid state physics<sup>35</sup>. Here in fact one needs to describe the metallic state of the current/voltage electrodes, the molecular state of the actual device and magnetism on the same footing. In addition since a transport prob-

lem is essentially a non-equilibrium problem, variational principles are not valid. One cannot depend on the free energy for atomic relaxation and the full dynamics must be considered<sup>36</sup>. Finally detailed information about the elementary excitations (phonons, spin waves etc.) and the exact atomic positions are essential.

The aim of this review is to offer a complete overview of the fascinating field of molecular-spintronics. In particular we will demonstrate that a quantitative theory of quantum transport can offer important insights and can be an invaluable tool for understanding complicated experiments and for novel device designing. The paper is organized as follows. In the first two sections we will introduce the two fields of spin- and molecular-electronics. Then we will introduce the main computational tools, and we will discuss the latest progresses with molecular spin-valves. Finally we will overview the most recent and controversial findings, namely transport in molecular magnets,  $d^0$  ferromagnetism and contact induced ferromagnetism.

## II. SPIN-ELECTRONICS

### A. Transition metals and spin valves

Magnetic transition metals and their permalloys occupy an important place in the field of spin-electronics. This is essentially due to their generally high Curie temperature (for a commercially useful magnetic materials it must exceed  $\sim 500$  °K<sup>37</sup>), and the possibility of engineering the various magnetic properties by alloying. The ferromagnetism in  $3d$  transition metals can be understood by simply looking at their electronic structure.

The nominal atomic configurations of Ni, Co and Fe are respectively  $4s^23d^8$ ,  $4s^23d^7$  and  $4s^23d^6$ . Therefore in forming a solid one expects the Fermi level ( $E_F$ ) to be in a region of density of states (DOS) with dominant  $d$  character. Since the  $d$  shells are rather localized the DOS is extremely large around  $E_F$  and the material becomes Stoner unstable thus developing a ferromagnetic ground state. The band energies  $\epsilon_{\vec{k}\sigma}$  for the two different spin orientations ( $\sigma = \uparrow, \downarrow$ ) are shifted with respect to each other by a constant  $\Delta = \epsilon_{\vec{k}\downarrow} - \epsilon_{\vec{k}\uparrow}$ , with  $\Delta$  approximately 1.4 eV in Fe, 1.3 eV in Co and 1.0 eV in Ni. More sophisticated DFT calculations show that such picture is a good approximation of the real electronic structure of Ni, Co and Fe.

In addition to the formation of a net magnetic moment a consequence of the bandstructure spin-splitting is that the Fermi surface for the two spin directions is rather different. This difference is more pronounced in the case of strong ferromagnet, where only one of the two spin-split  $d$  manifolds is fully occupied (majority band) while the other has some fractional occupation (minority band). An example of this situation is fcc Co (the high temperature phase), whose electronic structure is presented in figure 1.

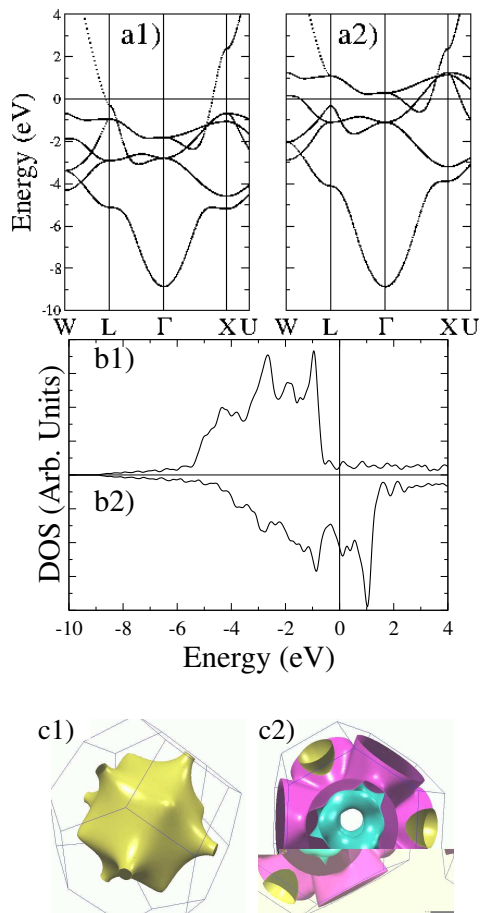


Figure 1: a) Band structure, b) density of states, and c) Fermi surface for fcc Co. The figures a1), b1) and c1) refers to the majority spin electrons, while a2), b2) and c2) to the minority. The pictures a) and b) have been obtained with density functional theory using the code SIESTA<sup>38</sup>, and c) from an *spd* tight-binding Hamiltonian<sup>39</sup>.

The main feature of the bandstructure of Co (and indeed of the other *3d* magnetic transition metals) is the presence of a broad (delocalized) and only weakly spin-split *s* band, and of a narrow (localized) and largely spin-split *d* band. The former has almost free electron-like character for energies both below (note the parabolic behavior of the bands around  $\Gamma$  for  $E \sim -9$  eV) and above  $E_F$ . In contrast the latter is only about 5 eV wide and cuts close to the Fermi level. Because of the spin-splitting of the *d* manifold,  $\Delta$ , the majority spin band has an almost spherical Fermi surface (see figure 1c1), while the minority one has a rather complicated structure, mostly arising from the *d* manifold (see figure 1c2). The different structure of the Fermi surface for majority and minority spins and the fact that these differences arise from a different orbital character are the main ingredients for understanding the transport properties of magnetic transition metal heterostructures.

Importantly the effects of alloying can be understood in the context of a rigid-band model, by shifting the Fermi level according to the valence of the dopant<sup>40,41</sup>. Finally it is worth mentioning that there are materials that at the Fermi level present a finite DOS for one spin specie and a gap for the other. These are known as half-metals<sup>42</sup> and are probably among the best candidates as materials for future magneto-electronics devices.

## B. Spin valves

The prototype of all spin devices is the spin-valve. This is formed by two magnetic layers (normally transition metals) separated by a non-magnetic spacer (either metal or insulator). One of the two magnetic layers is free to rotate in tiny magnetic fields, while the other usually is pinned by exchange coupling with an antiferromagnet or by strong magnetic anisotropy. The current passing through a spin-valve depends over the mutual orientation of the two magnetic layers and it is typically higher for a parallel alignment (PA) than for an antiparallel (AA). Thus a spin-valve behaves essentially as a spin polarizer/analyzer device. The quantity that defines the effectiveness of the spin-filtering effect is the GMR ratio  $R_{\text{GMR}}$  defined as (“optimistic definition”)

$$R_{\text{GMR}} = \frac{I_{\text{PA}} - I_{\text{AA}}}{I_{\text{AA}}}. \quad (1)$$

An alternative definition (“pessimistic definition”) using  $I_{\text{PA}} + I_{\text{AA}}$  as normalization is sometime used.

An intuitive understanding of the spin-filtering produced by a spin-valve can be obtained by looking at the Fermi level lineup of the materials forming the device. Let us consider for example a Ni/Cu/Ni spin-valve (see figure 2), and assume that the two spin-bands do not mix. This is the two spin fluid approximation, which is valid in the case of weak spin-orbit scattering and collinear magnetism<sup>43</sup>.

In the AA a spin electron propagates in the majority spin band in one layer and in the minority band in the other. Consequently electrons always travel across the Fermi surfaces of Cu and of both the spin-bands of Ni. In contrast in the PA the two spin currents are rather different. The majority current is made from electrons that have traveled within the Fermi surfaces of Cu and that of the majority spin of Ni, while the down spin current from electrons that have traveled within the Fermi surfaces of Cu and that of the minority spin of Ni. This leads to two different current paths for the AA and the PA. Since the two spin currents add to form the total current and since generally the resistances of majority and minority electrons are different in a magnetic transition metal, the current passing through the PA and AA configurations are different. Importantly the larger is the mismatch between the two spin currents, the larger in the GMR ratio.

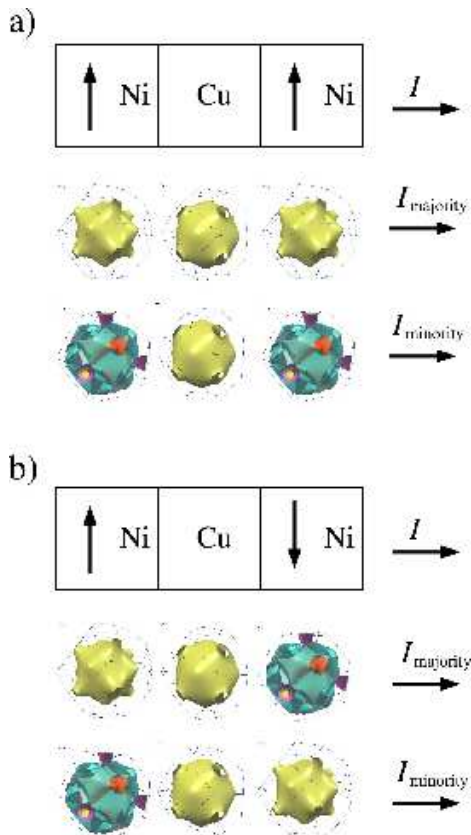


Figure 2: Magnetoresistance mechanism in a Ni/Cu/Ni spin valve in the two spin fluid approximation. In the parallel case a) the resistance of the majority spin channel is low since there is good match of the majority Fermi surfaces across the entire device. In contrast in the antiparallel state b) the alignment of the Fermi surface is such to have one high resistance interface for both the spin channels. This is given by the interface between the minority spin band of Ni and that of Cu. The formation of high resistance channels for both spins in the AA is responsible for the GMR effect.

### C. Spin polarization of a device

An important question is how to quantify the relative difference between the two spin currents in a magnetic device and how to relate this properties to the elementary electronic structure of the materials forming the device. We then define the spin-polarization  $P$  of a material/device as

$$P = \frac{I_{\uparrow} - I_{\downarrow}}{I_{\uparrow} + I_{\downarrow}}, \quad (2)$$

where  $I_{\sigma}$  is the spin- $\sigma$  contribution to the current.  $I_{\sigma}$  and  $P$  are not directly observable and must be calculated or inferred from indirect measurements. Unfortunately the way to relate the spin-current  $I_{\sigma}$  to the electronic structure of a material is not uniquely defined and depends on the particular experiment carried out.

As brilliantly pointed out by Mazin<sup>44</sup>, the relation be-

tween the spin-polarization of a magnetic material and its electronic structure depends critically on the transport regime that one is considering (ballistic, diffusive, tunneling ..). As a first approximation the current  $I$  is simply proportional to  $N_{\text{F}} v_{\text{F}}^n$ , where  $N_{\text{F}}$  and  $v_{\text{F}}$  are the DOS at the Fermi level and the Fermi velocity respectively. Different transport regimes weight the contribution of the Fermi velocity differently, and one has  $n = 2$  for diffusive transport,  $n = 1$  for ballistic transport and  $n = 0$  for tunneling.

Therefore the spin-polarization  $P$  becomes

$$P_n = \frac{N_{\text{F}}^{\uparrow} (v_{\text{F}}^{\uparrow})^n - N_{\text{F}}^{\downarrow} (v_{\text{F}}^{\downarrow})^n}{N_{\text{F}}^{\uparrow} (v_{\text{F}}^{\uparrow})^n + N_{\text{F}}^{\downarrow} (v_{\text{F}}^{\downarrow})^n}. \quad (3)$$

Typical values of  $P_n$  for several magnetic metals are reported in table I.

	$P_n$ (%)		
	$n=2$	$n=1$	$n=0$
Fe	20	30	60
Ni	0	-49	-82
CrO <sub>2</sub>	100	100	100
La <sub>0.67</sub> Ca <sub>0.33</sub> MnO <sub>3</sub>	92	76	36
Tl <sub>2</sub> Mn <sub>2</sub> O <sub>7</sub>	-71	-5	66

Table I: Spin-polarization of typical magnetic metals according to the various definitions given in the text. The data are taken from literature as follows: Ni and Fe<sup>44</sup>, CrO<sub>2</sub><sup>45</sup>, La<sub>0.67</sub>Ca<sub>0.33</sub>MnO<sub>3</sub><sup>46</sup> and Tl<sub>2</sub>Mn<sub>2</sub>O<sub>7</sub><sup>47</sup>.

Importantly the spin-polarization of a device can be different from that of the materials forming it. This is connected to the fact that the bonding at the interface between two different materials can be strongly spin-selective. For instance if the bonding between two materials has mainly  $s$ -character, then one expects strong scattering for  $d$ -like electrons. As a consequence the spin-polarization of the current will be determined by the spin-polarization of the almost free  $s$ -electrons. This is usually much smaller than that of the  $d$ -electrons and it may even have the opposite sign. For instance it is demonstrated that the sign of the magnetoresistance of a magnetic tunneling junction can be altered by simply replacing the insulator forming the barrier<sup>48</sup>.

## III. MOLECULAR-ELECTRONICS

### A. Electrons transport through molecules

Transport through molecules and in general through low dimensional objects is somehow different than that in standard metals or semiconductors. This is substantially due to the collapse of the Fermi surface into a single energy level (the highest occupied molecular orbital - HOMO). The nature and lineup of the HOMO with

the Fermi energy of the current/voltage probes determine most of the transport properties. Let us consider the simple case of a two probe device. Following a simple model proposed by Datta<sup>49</sup> the typical energy level lineup is schematically presented in figure 3.

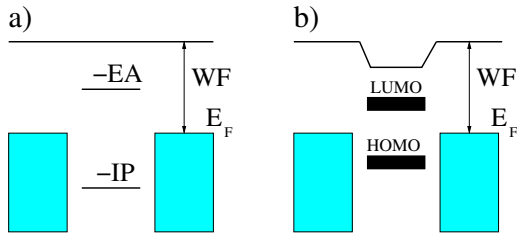


Figure 3: Energy level lineup between a molecule and two current voltage probes. In the weak coupling limit a) the molecule is characterized by the ionization potential (IP) and the electron affinity (EA), which line up with the metal Fermi energy (WF is the work function of the contact). In the case of strong coupling b) between the molecule and the leads the molecular levels shift and broaden. It is then more appropriate to discuss transport in terms of HOMO and LUMO states.

In absence of any coupling (figure 3a) both the energy levels of the molecule and the Fermi level of the electrodes will align with a common vacuum level. In this case the system is characterized by the work function of the electrodes and both the ionization potential (IP) and the electron affinity (EA) of the molecule. In this setup the molecule can exchange electrons with the electrodes only if the typical temperature is comparable to either IP-WF or WF-EA, a condition which is normally not satisfied. This guarantees local charge neutrality of the whole system and integer occupation of the molecule.

In contrast, the interaction between the molecular levels and the extended wave-functions of the metallic contacts has the effect of broadening and shifting the molecular levels. In the extreme limit of large coupling extended states spanning through the entire system (electrode plus molecule) can develop and the molecular device will behave as a good metal. In this limit the molecular levels cannot be associated any longer to the elementary removal energies of the isolated molecule and a description in terms of fractionally occupied HOMO and LUMO (lowest unoccupied molecular orbital) is more appropriate.

The transition from integer to fractional occupation of the molecule somehow depends on the typical molecular charging energy (say the EA) compared to the hopping integral  $\Gamma$  between the molecule and the contacts ( $\Gamma/\hbar$  is the escape rate from the molecule to the contacts). One has integer occupation if  $EA \gg \Gamma$  and metallic-like behaviour when  $\Gamma \gg EA$ . This is essentially the same physics leading to Mott metal-insulator transition in solid state. An electronic structure theory capable of exploring on the same footing all the intermediate situations between the strong and weak coupling limit is still not

available unless at prohibitive computational costs<sup>35</sup>.

The effect of an applied bias  $V$  is that of shifting the chemical potentials of the two current/voltage probes relative to each other by  $eV$ , with  $e$  the electronic charge. As a rule of thumbs current will flow whenever a molecular level (either the HOMO or the LUMO) is positioned within such a bias window. The appearing of molecular levels in the bias window when the potential is increased typically leads to changes in the slope of the  $I$ - $V$  characteristics, in steps in the differential conductance  $dI/dV(V)$  and in peaks in its derivative  $d^2I/dV^2(V)$ . This means that fingerprints of the molecular spectrum can be found in the measurement of its electrical properties. The same is true for the molecular elementary excitations, and peaks in  $d^2I/dV^2(V)$  can be found in correspondence of the energy of relevant phonon modes<sup>50</sup>.

## B. The bonding with the contacts

One of the fundamental aspects of molecular electronics is that the bonding between a molecule and the current/voltage probes can be engineered to a degree usually superior to that achievable in conventional inorganic heterostructures. This can dramatically change the current flowing through a device. Consider for instance the simple case of an atomic gold chain, described by  $s$  orbitals only, sandwiching a  $\pi$ -bonded molecule (see figure 4).

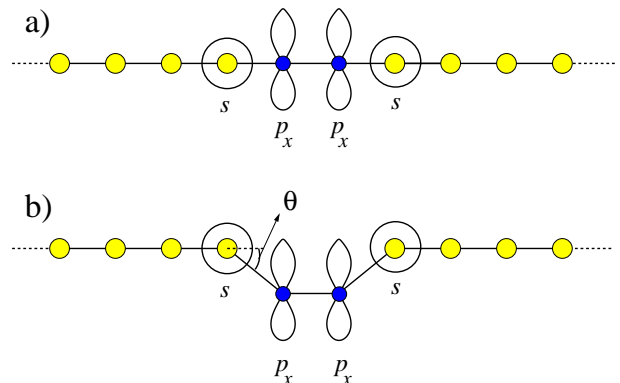


Figure 4: Au atomic chain sandwiching a  $\pi$ -bonded molecule (say an  $S_2$  molecule). a) the molecule is aligned with the Au chain and the transmission is suppressed because the matrix element  $\langle s|H|p_x \rangle$  vanishes. In contrast when the molecule forms some angle  $\theta$  with the Au chain b) then a component of the hopping integral along the bond develops and current can flow.

Let us assume that the relevant molecular state (the one close to the Fermi level of the gold chain) is formed by  $p_x$  orbitals, i.e. those perpendicular to the chain axis. When the molecule is positioned along the axis of the chain the hopping integral between the molecule and the chain  $\langle s|H|p_x \rangle$  vanishes regardless of the separation between the two. This is simply the result of the particular symmetry of the problem since  $s$  and  $p_x$  orbitals do

not share the same angular momentum about the bond axis<sup>51</sup>. As a consequence the current is identically zero.

In contrast if the molecule is not coaxial to the chain (figure 4b), then there is a component of the  $p_x$  orbital along the bond axis and the hopping integral becomes  $\gamma_{sp\sigma} \sin\theta$ , where  $\gamma_{sp\sigma}$  is the  $sp\sigma$  hopping integral and  $\theta$  the bond angle. This dependence of the bonding on the bond orientation may have dramatic consequences on the  $I$ - $V$  characteristics. In figure 5 we present the  $I$ - $V$  curve for the system of figure 4 calculated with a self-consistent tight-binding model where it is assumed a linear dependence of the on-site energies over the orbital occupation (see reference [35] for details).

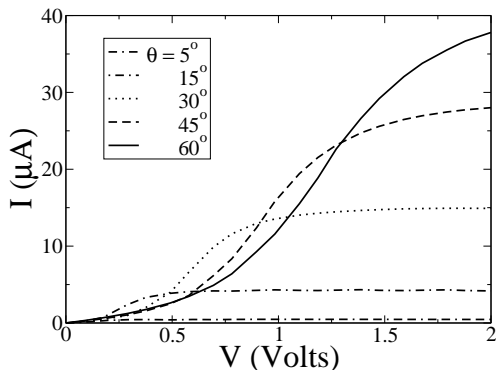


Figure 5:  $I$ - $V$  characteristics for a  $S_2$  molecule sandwiched between two semi-infinite gold chains (see figure 4). The curves are calculated using the tight-binding based non-equilibrium Green function method of reference<sup>35</sup> with the following parameters:  $\epsilon_{Au}=-5.9$  eV,  $\epsilon_S=-6.15$ eV eV,  $\gamma_{ss\sigma}=-3.0$  eV,  $\gamma_{sp\sigma}=1.52$  eV,  $\gamma_{pp\pi}=-0.98$  eV,  $U_{Au}=-6.7$  eV and  $U_S=-6.15$  eV.  $\epsilon$  is the on-site energy,  $\gamma$  hopping integral and  $U$  the charging energy.

From figure 5 it is clear that the  $I$ - $V$  characteristics of a molecule can be largely engineered by simply changing the details of the bonding with the electrodes. This is considerably more complicated in extended interfaces (for instance between two metals), since disorder, interdiffusion and roughness have the effect of averaging out the atomistic details of the bonding. It is important to remark that even when molecular layers are grown a good level of tuning of the bonding properties still exists. For instance the bonding site and the bond angle usually depend on the layer density (coverage)<sup>52</sup>, and these can be further tuned by changing the end groups.

### C. Why spins and molecules?

What are the advantages of using molecules instead of inorganic materials for performing spin-physics? These are essentially two. On the one hand there are intrinsic molecular properties and in particular the weak spin-orbit and hyperfine interactions. On the other hand there

are the properties connected to the formation of interfaces between magnetic metals and molecules. We will return to the interfacial properties in the next sections, here we focus our attention only on the intrinsic aspects.

Spin-orbit interaction is a relativistic effect which couples the electron spin  $\vec{S}$  with its angular momentum  $\vec{L}$ . The spin-orbit Hamiltonian in general can be written as  $H_{SO} = V_{SO}\vec{S} \cdot \vec{L}$ , where  $V_{SO}(\vec{r})$  is a term which contains the gradient of the electrostatic potential. Although it is rather intuitive to realize that the strength of this interaction grows with the atomic number  $Z$  (it is proportional to  $Z^4$ ), its actual value in the solid state depends on various factors such as the crystal symmetry and the material composition. Importantly the spin-orbit effect is responsible for spin-precession and the loss of spin-coherence. In organic materials usually the spin-orbit interaction is rather small. This is mostly due to the small atomic number of carbon. In table II we compare the spin-orbit splitting  $\Delta_{SO}$  of the valence band of several semiconductors<sup>53</sup> with that of carbon diamond<sup>54</sup>. The

	$\Delta_{SO}$ (meV)
Si	44
Ge	290
GaAs	340
AlAs	280
InAs	380
GaP	80
InP	111
GaSb	750
AlSb	670
InSb	980
C	13

Table II: Valence band spin-orbit splitting for various semiconductors.

table shows that in carbon the spin-split of the valence band is approximately one order of magnitude smaller than in ordinary III-V or group IV semiconductors and one should expect a considerably longer spin-lifetime<sup>6,7</sup>.

Another important interaction, which generally leads to spin-decoherence, is the hyperfine interaction between electron and nuclear spins. This has the form

$$H_{\text{hyp}} = A_{\text{hyp}} \vec{s} \cdot \vec{S}_N, \quad (4)$$

where  $\vec{s}$  and  $\vec{S}_N$  are respectively the electronic and nuclear spin, and  $A_{\text{hyp}}$  is the hyperfine coupling strength. Similarly to the case of spin-orbit, also hyperfine interaction is a source of spin de-coherence<sup>55</sup>, since the random flipping of a nuclear spin can cause that of an electron spin. However, in III-V semiconductors hyperfine interaction was also proved to be a tool for controlling nuclear spins via optically polarized electron spins<sup>56</sup>. In organic materials usually the hyperfine interaction is weak. The main reason for this is that most of the molecules used

for spin-transport are  $\pi$ -conjugate molecules where the transport is mostly through molecular states localized over the carbon atoms. Carbon, in its most abundant isotopic form,  $^{12}\text{C}$ , has nuclear spin  $S_{\text{N}}=0$ , and therefore is not hyperfine active. Moreover the  $\pi$ -states are usually delocalized and  $H_{\text{hyp}}$  can be anyway rather small. In table III we report the value of the nuclear spin for various atomic species with their relative isotopic abundance.

Isotope	IA (%)	$S_{\text{N}}$
$^1\text{H}$	99.98	1/2
$^2\text{H}$	0.02	1
$^{12}\text{C}$	98.93	0
$^{13}\text{C}$	1.1	1/2
$^{14}\text{N}$	99.632	2
$^{15}\text{N}$	0.368	1/2
$^{16}\text{O}$	99.757	0
$^{18}\text{O}$	0.205	0
$^{19}\text{F}$	100	1/2
$^{69}\text{Ga}$	60.108	3/2
$^{71}\text{Ga}$	39.892	3/2
$^{75}\text{As}$	100	3/2
$^{28}\text{Si}$	92.2297	0
$^{29}\text{Si}$	4.6832	1/2
$^{30}\text{Si}$	3.0872	0

Table III: Nuclear spin for elements present in typical organic molecules and in both Si and GaAs. Here we report the nuclear spin for the most abundant isotopes, together with their relative isotopic abundance (IA).

Estimates of the spin-lifetime of organic materials from transport experiments are at the moment only a few. Moreover in most cases these are extracted from spin-valves measurements by fitting to the Jullier's formula<sup>57</sup>. This procedure does not distinguish the source of spin-flip, which may not be located inside the molecule, but at the interface with the magnetic electrodes. Therefore these measurements are likely to offer a conservative estimate of the spin-lifetime. Nevertheless the values of the spin diffusion length reported in the literature are rather encouraging for carbon nanotubes (130nm)<sup>20</sup>, polymers (200nm)<sup>23</sup>, or Alq<sub>3</sub> molecules (5nm)<sup>58</sup>.

Finally a conclusive note needs to be made on conducting polymers. These are extremely attractive materials since their electrical conductivity can be changed by over twelve orders of magnitude with the chemical or electrochemical introduction of various counterions<sup>59</sup>. Spin-dynamics in polymers has been extensively studied with EPR spectroscopy<sup>60</sup> and it is largely dominated by the presence of paramagnetic centers in the form of free radicals, ion-radicals, molecules in triplet states and transition metal complexes. Even more interesting is the fact that the elementary excitations leading to electron transport are not band-like but usually involve lattice vibrations, and most importantly some of them are spin-

polarized.

For instance in the *trans*-isomer of polycetylene the Su-Schrieffer-Heeger theory<sup>59</sup> predicts a soliton-like transport mechanism. This has a peculiar spin-charge relationship, since a neutral soliton corresponds to a radical with spin 1/2, while both negatively and positively charged solitons are spinless and diamagnetic. The study of spin-transport in devices made by transition metals in contact with such polymers is potentially extremely interesting. This is because of the proximity of two fundamentally different ground states, one electronically correlated (the magnetic material), and one with strong correlation between electronic and vibrational degrees of freedom (the polymer). The investigation, both experimentally and theoretically, of these combined systems is in its infancy<sup>61</sup>.

## IV. QUANTITATIVE TRANSPORT THEORY

### A. Simple Model

Modern theory of quantum transport is based on scattering theory in conjunction with accurate electronic structure methods. Although this approach has recently come to question, in particular in the case of electrons interacting beyond the mean-field level<sup>62</sup>, it still remains the most versatile and scalable available. In addition its foundations are extremely intuitive and simple. Let us start our discussion by presenting a simple model, first introduced by Datta<sup>49</sup>, which already contains all the elements of a more formal and accurate theory.

Consider a given molecule attached to two current/voltage probes kept at two different chemical potentials  $\mu_{\alpha}$ , with  $\alpha=L$  (left), R (right). The leads are assumed featureless, which is with a constant DOS. The molecule is described by an energy level  $\epsilon$  (say the HOMO), coupled to the current/voltage probes by the hopping integrals  $t_{\alpha}$  ( $\alpha=L, R$ ). The density of states associated to such a state is

$$D_{\epsilon}(E) = \frac{t/2\pi}{(E - \epsilon)^2 + (t/2)^2}, \quad (5)$$

where the level lifetime  $\hbar/t$  is determined by the coupling with the leads only  $t = t_L + t_R$ . Both the current  $I$  flowing through the molecular state and state occupation  $N$  can be determined by balancing the in-going and out-going fluxes and read

$$I = \frac{e}{\hbar} \int_{-\infty}^{+\infty} dE D_{\epsilon}(E) \frac{t_L t_R}{t} [f_L(E) - f_R(E)], \quad (6)$$

and

$$N = \int_{-\infty}^{+\infty} dE D_{\epsilon}(E) \frac{t_L f_L(E) + t_R f_R(E)}{t}, \quad (7)$$

where  $f_{\alpha}(E) = \frac{1}{1 + e^{(\epsilon - \mu_{\alpha})/k_B T}}$  is the Fermi distribution of the contact  $\alpha$ . From the equations above it is clear that

current will flow only (at least for small broadening and low temperature) if the energy level is in between the chemical potentials of the two leads. With no external bias these are identical, but when a potential  $V$  is applied then  $\mu_L - \mu_R = eV$  and current will flow.

In general  $\epsilon$  depends on the details of the electronic structure of the system. As a simple approximation we may assume it is a function of the level occupation only  $\epsilon = \epsilon(N)$ . This suggests a simple self-consistent procedure where  $\epsilon(N)$  and the equation (7) are solved iteratively before the current is evaluated with the (6).

Spin can be easily introduced in this simple model in the two spin fluid approximation. Since the two spin channels do not mix the equations (6) and (7) can be replaced by two pairs of equations for the spin-resolved molecular level occupation  $N^\sigma$  and the spin-current  $I_\sigma$ . In a similar way the molecular level can also be spin-polarized  $\epsilon \rightarrow \epsilon^\sigma$  and it may depend of the spin density instead of the density only  $\epsilon^\sigma(N^\uparrow, N^\downarrow)$ . Importantly in the case where the current/voltage probes are ferromagnetic spin-degeneracy is lifted by introducing spin-dependent hopping integrals  $t_\alpha^\sigma$  between the leads and the molecule. These however capture the fact that majority and minority electrons couple to the molecule in a different way, but not that the DOS for the different spin directions in a ferromagnet is different. For this last feature a more detailed description of the electronic structure of the leads is needed.

## B. *Ab initio* methods

The non-equilibrium Green's function (NEGF) method is by far the most used among all the quantum transport schemes. Although it is based on very rigorous ground<sup>63</sup> it can be understood as the natural extension of the toy-model discussed in the previous section. The general idea is to divide a two probe device into three regions: two current/voltage probes and a scattering region. The criterion for this fragmentation is that the scattering region is the portion of the device where the potential drops. Its boundaries are defined by the condition that the charge density matches exactly that of the bulk material forming the leads (see reference<sup>27</sup> for a more detailed description).

Let us assume that the problem can be formulated over some sort of localized basis set, and therefore the Hamiltonian for the whole system (scattering region plus leads) is simply an infinite hermitian matrix. The central quantity, which replaces the simple density of states  $D_\epsilon(E)$ , is the non-equilibrium Green's function for the scattering region  $G(E)$

$$G(E) = \lim_{\eta \rightarrow 0} [(E + i\eta) - H_S - \Sigma_L - \Sigma_R]^{-1}. \quad (8)$$

This is the Green's function associated to the Hamiltonian  $H_S + \Sigma_L + \Sigma_R$ , which is composed by the Hamiltonian of the scattering region  $H_S$  and the self-energies  $\Sigma_L$  and  $\Sigma_R$ .

Note that if one assumes that  $H_S$ ,  $\Sigma_L$  and  $\Sigma_R$  are just C-numbers, then  $i[G(E) - G^*(E)]$  is  $D_\epsilon(E)$  for  $\epsilon \rightarrow H_S$  (real) and  $t_\alpha/2 \rightarrow \Sigma_\alpha$  (purely imaginary). Thus the self-energies can be associated with the interaction between the scattering region and the current/voltage probes. In practice they can be written as  $\Sigma_L = H_{LS}^\dagger g_L H_{LS}$  and  $\Sigma_R = H_{RS} g_R H_{RS}^\dagger$ , with  $H_{\alpha S}$  the coupling matrix between the leads  $\alpha$  and the scattering region.  $g_\alpha$  are the surface Green's functions for the leads, i.e. the Green's function for a semi-infinite lead evaluated at the termination plane<sup>64</sup>. Thus the self-energies contain information on both the coupling between the scattering region and the electrodes and on the electronic structure of the leads themselves.

The crucial point is that both the two-probe current  $I$  and the density matrix associated to the scattering region  $\rho$  can be obtained from the Green's function  $G(E)$

$$I = \frac{e}{h} \int_{-\infty}^{+\infty} dE \text{Tr}[G \Gamma_L G^\dagger \Gamma_R] [f_L(E) - f_R(E)], \quad (9)$$

and

$$\rho = \frac{1}{2\pi} \int dE G [\Gamma_L f_L + \Gamma_R f_R(E)] G^\dagger, \quad (10)$$

where  $G = G(E)$ ,  $\Gamma = \Gamma(E)$  we have now introduced the broadening matrices

$$\Gamma_\alpha = i[\Sigma_\alpha - \Sigma_\alpha^\dagger]. \quad (11)$$

Equations (8) and (9) allow us to calculate the current once the Hamiltonian for the scattering region and the self-energies are given. Unfortunately these are not known *a priori*, since they require the evaluation of the electronic structure of an infinite non-periodic system. However their calculation do not require the actual solution of this open system and the notion of locality (the same that allows us to separate the leads from the scattering region) can be efficiently used. The self-energies in fact involve only bulk quantities, i.e. quantities which can be evaluated from a bulk calculation for a periodic system. In addition a self-consistent scheme can be designed for evaluating  $H_S$ . The crucial point here is to assume that the whole electronic structure can be described by a single-particle theory, in such a way that  $H_S$  depends only on the density matrix  $H_S = H_S[\rho]$ . This is for instance the case of DFT or Hartree-Fock methods. Hence  $H_S[\rho]$  and the equations (8) and (10) can be iterated self-consistently until convergence, and then the current can be evaluated with equation (9). This scheme, with differences concerning the specific numerical implementation, is used by most of the DFT-based NEGF packages available at present<sup>27,28,29,30,31,32,33</sup>.

Also in this case the addition of spin polarization does not bring any fundamental changes in the formalism. In the simple case of collinear-spins, then all the quantities introduced (Green's functions, charge density, Hamiltonian, self-energies ...) becomes block diagonal matrices



in spin space. The Hamiltonian now depends on both the charge density and the magnetization as in standard spin-polarized mean field electronic structure methods. Importantly the current is still carried in parallel by the two spin species. In the more complicated case of non-collinear spin (or if spin-orbit is present) then the off-diagonal blocks do not vanish and the current cannot be broken down into the majority and minority contributions.

Note that computationally the introduction of magnetism usually makes the calculation more complicated. First one needs to consider matrices larger than the unpolarized case. Secondly and most importantly the Hamiltonian matrix becomes considerably more sparse. In a ferromagnet in fact, for instance in a transition metal, the delocalized  $s$ -electrons responsible for most of the electron transport coexist with the tightly bound  $d$ -electrons, which provide the local magnetic moment. This means that most of the matrix elements between  $d$  orbitals located on atoms far from each other vanish, making the Hamiltonian more sparse than that of standard free-electron like metals (for instance Au). In the case of sparse matrices standard recursive methods for evaluating the self-energies become numerically unstable if not prohibitive, and more sophisticated schemes are needed<sup>27,28</sup>.

## V. MOLECULAR SPIN-VALVES

As pointed out in the introduction spin-valves are the prototypical spin-devices and therefore are the most studied architectures for spin-transport through molecules. The first prediction of a GMR-like effect in molecules is from Emberly and Kirczenow, who investigated the transport through a 1,4-benzenedithiolate molecule attached to Ni electrodes. Because of the problems of dealing with magnetic current/voltage probes mentioned in the previous section, this work and most of the early calculations<sup>65</sup> were limited to empirical models for the electronic structure.

A first step in the direction of using *ab initio* electronic structure methods was suggested by Pati and co-workers<sup>66,67,68</sup>, who considered a setup in which a given molecule is sandwiched between two magnetic ions, or clusters, which then are attached to non-magnetic electrodes (see figure 6).

This setup removes the problems connected with constructing the self-energies for magnetic materials and a GMR-like effect is produced by the magnetic ions, which in turn are exchanged coupled through the molecule. Clearly the scheme is highly idealized. It essentially describes the transport through a magnetic molecule (molecule plus magnetic ions) from non-magnetic leads, and not that of a magnetic spin-valve. Importantly it does not account for both the spin-polarized DOS of the contacts and the accurate orbital character of the bonding between the molecule and the magnetic surfaces.

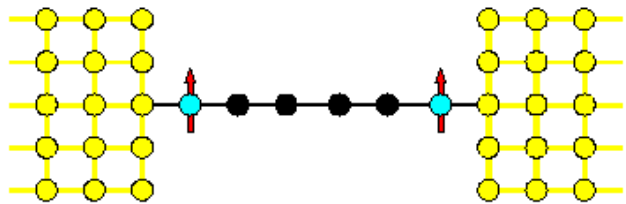


Figure 6: Setup for early molecular spin-valve calculations. A molecule (black circles) is sandwiched between two magnetic ions (blue circles), which are then contacted by two non-magnetic current/voltage electrodes. The red arrows indicate the local magnetic moments.

An interesting alternative, that still avoids the construction of magnetic leads, was proposed by Wei and co-workers<sup>69</sup>, who used Al leads locally immersed in a magnetic field. In this case the spin-polarization of the leads is achieved through simple Zeeman splitting and the direction of the local magnetic fields at the two contacts replaces that of the magnetic moments of a ferromagnet. In this case the DOS of the leads is spin-polarized, however the orbital nature of the bonding is identical for both majority and minority spins. Importantly most of these early calculations were ahead of experiments and largely inspired them.

### A. Metallic and tunneling junctions

The study of molecular transport with ferromagnetic contacts from first principles has a young history since only recently algorithms stable enough to deal with extremely sparse matrices and thus with magnetic leads were made available<sup>27,28</sup>. Here we describe the results obtained with the code *Smeago*<sup>27,28</sup> for both insulating and tunneling molecules.

As an example of different transport regimes, we consider spin-valves made from Ni leads and a molecular spacer which is either [8]-alkane-dithiolate (octane-dithiolate) or 1,4-[3]-phenyl-dithiolate (tricene-dithiolate). A schematic DOS and the charge density isosurfaces of the HOMO and LUMO states for the isolated molecules are presented in figures 7 and 8.

The two molecules present rather different characteristics. The HOMO-LUMO gap<sup>70</sup> is about 2.5 eV for tricene and almost double (5 eV) for octane. In addition while in tricene the charge density of the first two HOMO levels and the LUMO is extended over the whole molecule, in octane this is predominantly localized around the S atoms of the thiol groups. We then expect that the octane and the tricene will form respectively TMR and GMR devices, as actually found in our calculations<sup>27</sup>.

Let us consider octane first. The zero-bias transmission coefficient of the Ni/octane/Ni junction presents a sharp peak at  $E_F$  that scales exponentially with the

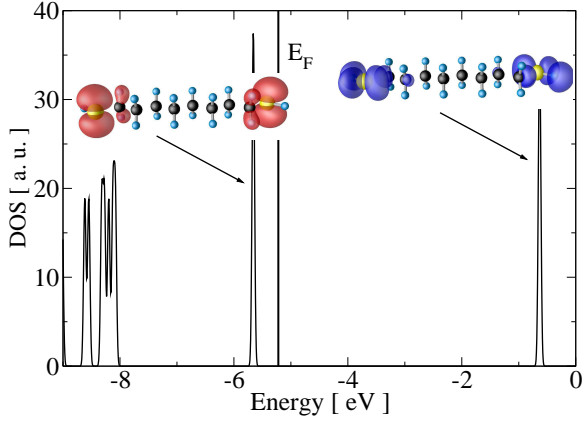


Figure 7: [8]-alkane (octane) molecule: DOS and charge density isosurface plots for the relevant molecular states of the isolated molecule.  $E_F$  denotes the position of the Fermi level for the isolated molecule.

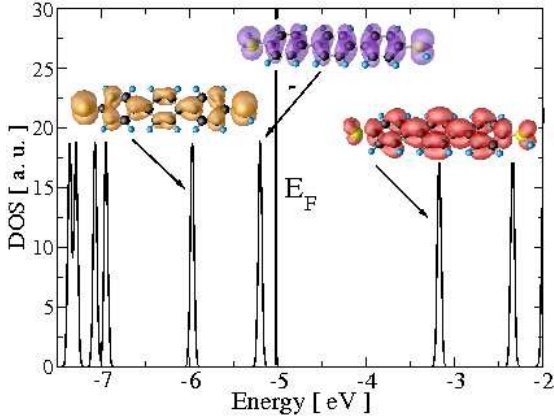


Figure 8: 1,4-[3]-phenyl (tricene) molecule: DOS and charge density isosurface plots for the relevant molecular states of the isolated molecule.  $E_F$  denotes the position of the Fermi level for the isolated molecule.

number of alkane groups  $T \propto e^{-\beta n}$  ( $\beta \sim 0.88$ ). This is demonstrated in figure 9 for the parallel configuration and confirms that device is in a tunneling regime. Note that the method is accurate down to a conductance of  $\sim 50$ pS. Interestingly the exponent is similar to that found for the same molecule attached to gold (111) surfaces<sup>71</sup>. The coupling between the thiol groups and the electrodes is strong and it gives rise to a small spin-polarization of the two S atoms. However since both the HOMO and LUMO states are strongly localized at the thiol groups, at the Fermi level there is no molecular state extending through the entire structure. Hence the Ni/octane/Ni junction presents the features of a TMR spin-valve.

The case of 1,4-[n]-phenyl-dithiolate is different, in particular we find that the current does not scale sensibly with the number of phenyl groups in the molecule. In fig-

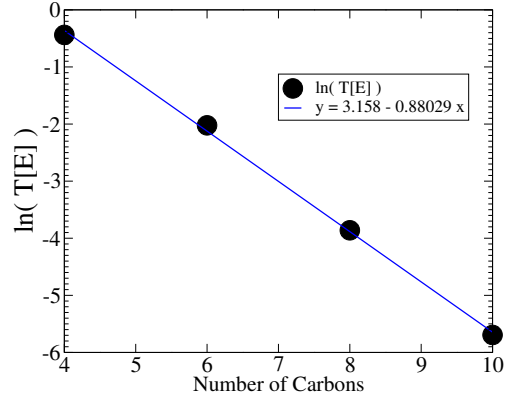


Figure 9:  $\ln(T(E_F))$  as a function of the number of C atom for [n]-alkane-dithiolate attached to Ni leads. The black circles correspond to our calculated values, and the solid line is our best linear fit. Here the spin-valve is in the parallel configuration.

ure 10 we present the transmission coefficient as a function of energy of 1,4-[n]-phenyl-dithiolate for 1, 3 and 4 phenyl rings when the magnetization vectors of the leads are parallel to each other. It is clear that, although there

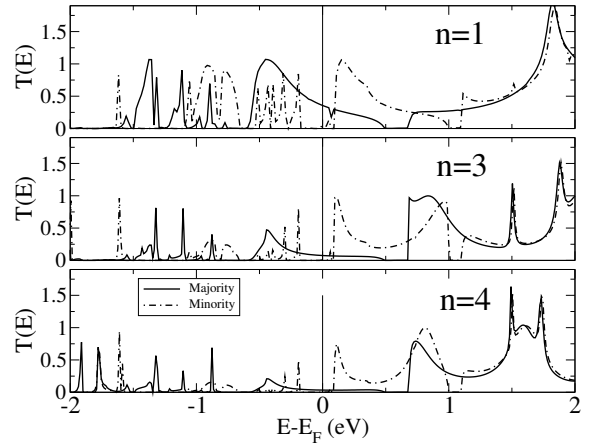


Figure 10: Transmission coefficient as a function of energy for 1,4-[n]-phenyl-dithiolate molecules with  $n=1, 3,$  and  $4$ . Here the spin-valve is in the parallel configuration. A similar scaling of the transmission coefficient as a function of  $n$  is found for the antiparallel configuration.

is a reduction of the transmission coefficient as a function of the number of rings, this remains close to unity for most of the energy range, and certainly there is not an exponential decay. Therefore in this class of molecules the transport seems to be appropriately described by a coherent resonant tunneling mechanism through extended molecular states.

This picture is enforced by the fact that the zero-bias transmission coefficient approaches unity for energies close to the leads Fermi level. In addition, from

the study of the evolution of the orbital resolved density of states as a function of the distance between the thiol group and the electrodes<sup>27</sup> we identify such a resonant state as the HOMO state of tricene. However it is worth mentioning that this appears rather broad and spin-split, because of the strong coupling with the  $d$  orbitals of the leads. In conclusion all this suggests that a Ni/tricene/Ni spin-valve behaves as metallic spin-valve.

The  $I$ - $V$  characteristics of both the molecules are strongly non-linear with the bias and consequently also the GMR ratio suffers this non-linearity. In figures 11 and 12 we present the  $I$ - $V$  curves, the GMR ratio and the zero-bias transmission coefficient for the two molecules.

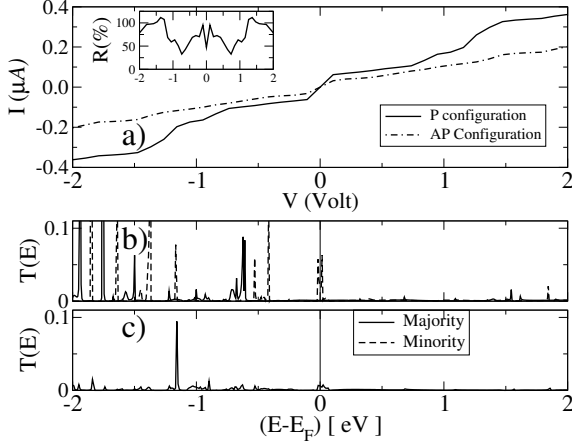


Figure 11: a)  $I$ - $V$  characteristic, and zero bias transmission coefficients for the b) parallel and c) antiparallel configuration of an octane-based Ni spin-valve. In the antiparallel case the transmission coefficient is identical for both the spin directions. In the inset we present the corresponding MR ratio.  $E_F$  is the position of the Fermi level of the Ni leads. From reference<sup>28</sup>.

Again consider octane first. Here the transmission coefficient at zero bias is dominated by a number of sharp peaks in the parallel configuration, which get considerably suppressed in the antiparallel one. In particular a minority peak appears at the Fermi level and it is mostly responsible for the low-bias conductivity. Such sharp peaks in the transmission coefficient are usually a signature of resonant states at the interface between the leads and the insulating media. At resonance they can carry a considerable current, however small bias and disorder are usually rather effective in suppressing their contribution to the current. Evidence for these surface states has been already provided for conventional magnetic tunneling junctions both experimentally<sup>72</sup> and theoretically<sup>73</sup>.

The  $I$ - $V$  characteristic is rather linear for the antiparallel configuration but presents a non-trivial slope for the parallel case. This gives rise to a non-monotonic dependence of the GMR ratio over the bias. Importantly both the layer resistance and the TMR ratio are in the same range as in recent experiments on octane-based Ni spin-valves<sup>21</sup>. However, a direct comparison with experiments

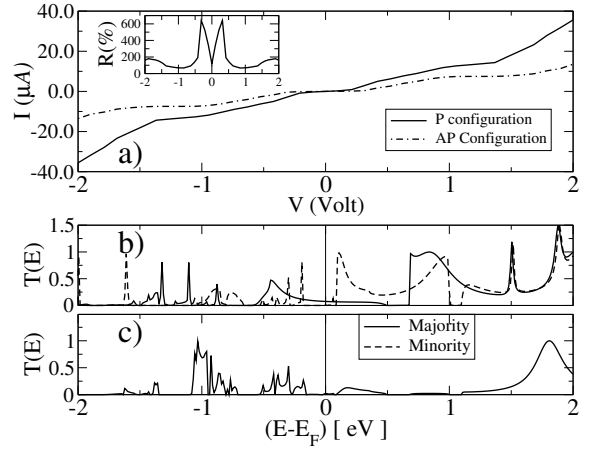


Figure 12: a)  $I$ - $V$  characteristic, and zero bias transmission coefficients for the b) parallel and c) antiparallel configuration of a tricene-based Ni spin-valve. In the antiparallel case the transmission coefficient is identical for both the spin directions. In the inset we present the corresponding MR ratio.  $E_F$  is the position of the Fermi level of the Ni leads. From reference<sup>28</sup>.

is difficult since the actual number of molecules bridging the two electrodes is not known with precision. Moreover a degradation of the GMR signal due to spin-flip and electron-phonon scattering, misalignment of the magnetization of the contacts and current shortcut through highly conductive pin-holes, can drastically reduce  $R_{\text{GMR}}$  in actual samples.

In contrast in the case of metallic (tricene) junctions the transmission coefficient at zero bias presents a much higher transmission and is a rather smooth function of the energy. In the parallel case most of the transmission at  $E_F$  is due to the majority spin, while the contribution of the minority is significant only for energies at about 200 meV above  $E_F$ . In the antiparallel configuration such transmission at the Fermi level is strongly suppressed and the resulting current is considerably lower. This produces an extremely large GMR ratio for small bias, exceeding 600%.

An interesting feature is that, in first approximation, the transmission coefficient at zero bias for the antiparallel state appears to be a convolution of those for the majority and minority spin in the parallel case. This finding can be qualitatively understood in terms of transport through a single molecular state (see figure 13). Let  $t^\uparrow(E)$  be the majority spin hopping integral from one of the leads to the molecular state, and  $t^\downarrow(E)$  the same quantity for the minority spins. Then, neglecting multiple scattering (i.e. all interference effects), the total transmission coefficients of the entire spin-valve in the parallel state can be written  $T^{\uparrow\uparrow}(E) = (t^\uparrow)^2$  and  $T^{\downarrow\downarrow}(E) = (t^\downarrow)^2$  respectively for the majority and minority spins. Similarly the transmission in the anti-parallel configuration is  $T^{\uparrow\downarrow}(E) = T^{\downarrow\uparrow}(E) = t^\uparrow t^\downarrow$ . Thus  $T^{\uparrow\downarrow}(E)$  is a convolu-

tion of the transmission coefficients for the parallel case  $T^{\uparrow\downarrow} \propto \sqrt{T^{\uparrow\uparrow}T^{\downarrow\downarrow}}$ .

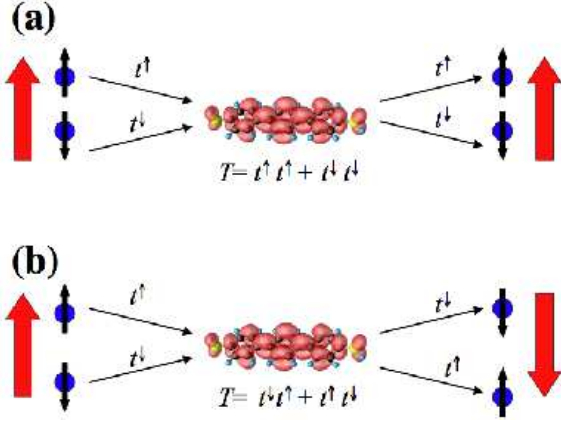


Figure 13: Scheme of the spin-transport mechanism through a single molecular state.  $t^{\uparrow}(E)$  ( $t^{\downarrow}(E)$ ) is the majority (minority) spin hopping integral from one of the leads to the molecular state. Neglecting quantum interference, in the parallel case (a) the total transmission coefficient is simply  $T = (t^{\uparrow})^2 + (t^{\downarrow})^2$ , while in the antiparallel (b)  $T = 2t^{\uparrow}t^{\downarrow}$ . Note that if either  $t^{\uparrow}$  or  $t^{\downarrow}$  vanishes, the current in the antiparallel configuration will also vanish (infinite GMR).

An extreme case is when only one spin couples to the molecular state. Then the total transmission in the antiparallel case is identically zero since either  $t^{\uparrow}$  or  $t^{\downarrow}$  vanishes. This is the most desirable situation in real devices since, in principle, an infinite  $R_{\text{GMR}}$  can be obtained. Note that in this situation the system leads+molecule behaves as a half-metal although the two materials forming the device are not half-metals themselves. An even more extreme situation is when for a particular energy window the transport is through two distinct molecular states, which are respectively coupled to the majority and minority spin only. This may happen for instance due a particular symmetry of the molecular anchoring groups. Then in this energy window one will find  $T^{\uparrow\uparrow}(E) \neq 0$ ,  $T^{\downarrow\downarrow}(E) \neq 0$  but  $T^{\uparrow\downarrow}(E) = 0$  (see figure 14).

The fact that in good approximation  $T^{\uparrow\downarrow} \propto \sqrt{T^{\uparrow\uparrow}T^{\downarrow\downarrow}}$  can be used for enhancing the GMR ratio. Consider for instance the case when  $T^{\uparrow\uparrow} \gg T^{\downarrow\downarrow}$ . Then we have  $T_{\text{P}} \approx T^{\uparrow\uparrow}$  and  $T_{\text{AP}} \approx \sqrt{T^{\uparrow\uparrow}T^{\downarrow\downarrow}}$  for the total transmission coefficients respectively of the parallel and antiparallel configurations. Clearly a reduction of  $T^{\downarrow\downarrow}$  will produce a considerable reduction in the transmission of the antiparallel alignment, leaving almost unchanged that of the parallel one. We have explored this avenue<sup>27</sup> by replacing the thiol group with either a Se or a Te atoms. These provide a rather strong bond, although generally the bond length is increased due to the larger atomic radius of the anchoring atom. The transmission,  $I$ - $V$  characteristics and GMR for 1,4-benzene anchored to Ni via S, Se or Te are presented in figures 15, 16 and 17. Clearly the pictures show a rather dramatic increase of the GMR

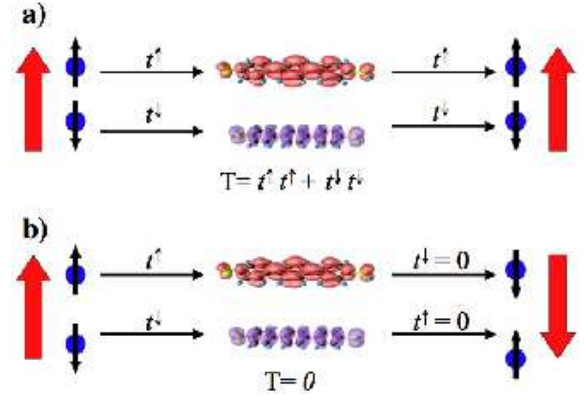


Figure 14: Scheme of the spin-transport mechanism through two energetically closely spaced molecular states. The first state (red) couples only to the majority spin band, while the minority spin couple only to the purple state. In the parallel case one finds  $T^{\uparrow\uparrow}(E) \neq 0$  and  $T^{\downarrow\downarrow}(E) \neq 0$  but in the antiparallel  $T^{\uparrow\downarrow}(E) = 0$ . We then expect an infinite GMR for such an energy window.

demonstrating that the GMR signal can be tuned by an appropriate choice of the anchoring chemistry.

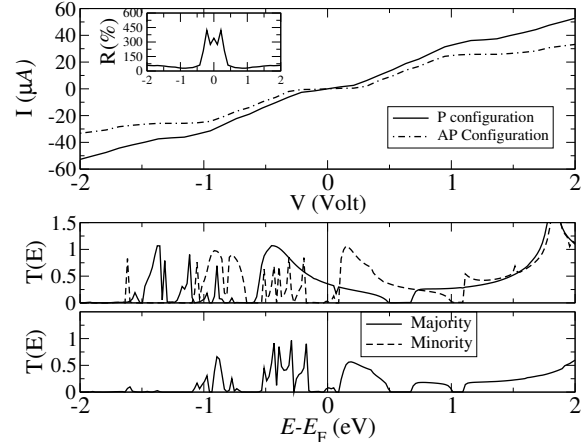


Figure 15: Transport properties for a 1,4-phenyl molecule attached to Ni (100) surfaces through a S group. The top panel shows the  $I$ - $V$  characteristics for both the parallel and antiparallel alignment of the leads and the inset the corresponding GMR ratio. The lower panel is the transmission coefficient at zero bias as a function of energy. Because of spin-symmetry, in the antiparallel case we plot only the majority spin. Reprinted with permission from<sup>27</sup> A.R. Rocha et al., Phys. Rev. B **73**, 085414 (2006). Copyright American Physical Society 2006.

Finally it is worth mentioning that a severe bias dependence of the GMR ratio, with also the possibility of negative values, has been recently predicted with either semi-empirical<sup>74</sup> and *ab initio*<sup>75</sup> methods.

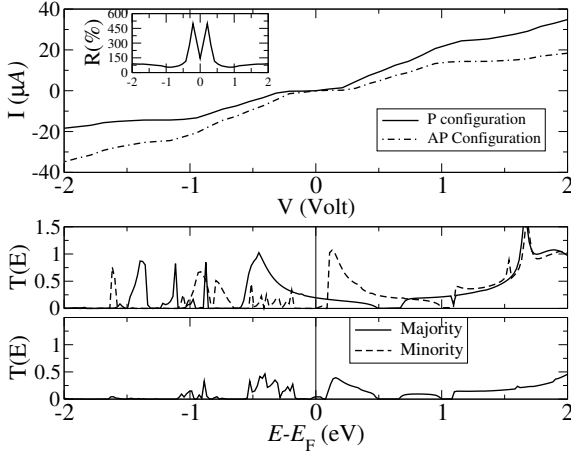


Figure 16: Transport properties for a 1,4-phenyl molecule attached to Ni (100) surfaces through a Se group. The top panel shows the  $I$ - $V$  characteristics for both the parallel and antiparallel alignment of the leads and the inset the corresponding GMR ratio. The lower panel is the transmission coefficient at zero bias as a function of energy. Because of spin-symmetry, in the antiparallel case we plot only the majority spin. Reprinted with permission from<sup>27</sup> A.R. Rocha et al., Phys. Rev. B **73**, 085414 (2006). Copyright American Physical Society 2006.

## B. Carbon Nanotubes

Carbon nanotubes are almost defect-free graphene sheets rolled up to form one-dimensional molecules with enormous aspect ratios<sup>76</sup>. Their conducting state (metallicity) depends on their chirality, however in the metallic configuration they are ideal conductors with a remarkably long phase-coherence length<sup>77,78</sup>. An important aspect is that the relevant physics at the Fermi level is entirely dominated by the  $p_z$  orbitals, which are radially aligned with respect to the tube axis. These include the bonding properties with other materials and between tubes. Therefore carbon nanotubes appear as an ideal playground for investigating both GMR and TMR through molecules. In fact one can expect that two tubes with different chirality will bond to a magnetic surface in a similar way, allowing us to isolate the effects of the molecule from that of the contacts. Indeed TMR-like transport through carbon nanotubes has been experimentally reported by several groups<sup>20,79,80,81,82,83,84,85</sup>.

Why would one expect a large GMR from a carbon nanotube? To answer this question we use an argument derived by Tersoff<sup>86</sup> and then subsequently refined<sup>87</sup> for explaining the contact resistance between a C-nanotube and an ordinary metal. Consider for simplicity an armchair nanotube (metallic). The Fermi surface of such tube consists only of two points, symmetric with respect to  $\Gamma$  in the 1D Brillouin zone (see figure 18). The Fermi wave-vector is then  $k_F = 2\pi/3z_0$  with  $z_0 = d_0\sqrt{3}/2$  and  $d_0$  the C-C bond distance ( $d_0=1.42$  Å).

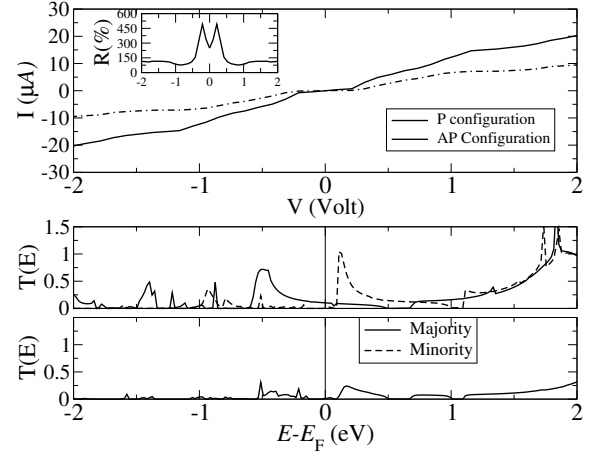


Figure 17: Transport properties for a 1,4-phenyl molecule attached to Ni (100) surfaces through a Te group. The top panel shows the  $I$ - $V$  characteristics for both the parallel and antiparallel alignment of the leads and the inset the corresponding GMR ratio. The lower panel is the transmission coefficient at zero bias as a function of energy. Because of spin-symmetry, in the antiparallel case we plot only the majority spin. Reprinted with permission from<sup>27</sup> A.R. Rocha et al., Phys. Rev. B **73**, 085414 (2006). Copyright American Physical Society 2006.

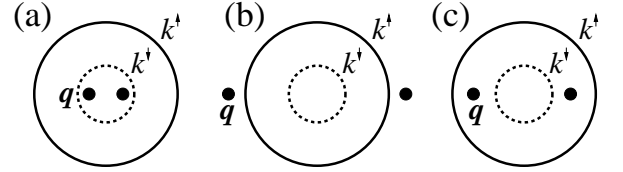


Figure 18: Fermi surfaces of an armchair carbon nanotube and of a magnetic transition metal. The Fermi surface of the nanotube consists in two points  $k_F^N = q$ , symmetric with respect to the  $\Gamma$  point. The Fermi surface of a transition magnetic metal consists of two spheres (for  $\uparrow$  and  $\downarrow$  spins) whose different diameters depend on the exchange field. The three possible scenarios discussed in the text: (a)  $q < k_F^\downarrow < k_F^\uparrow$ , (b)  $k_F^\downarrow < k_F^\uparrow < q$ , (c)  $k_F^\downarrow < q < k_F^\uparrow$ .

Assume now for simplicity that our magnetic metal is an exchange-split free-electron gas, whose band-energy is

$$E_k^\sigma = \frac{\hbar^2 k^2}{2m} + \sigma\Delta/2, \quad (12)$$

with  $\sigma = -1$  ( $\sigma = +1$ ) for majority (minority) spins and  $\Delta$  the exchange energy. The spin-dependent Fermi wave-vectors are then respectively  $k_F^\uparrow = \sqrt{2m(E_F + \Delta/2)}/\hbar$  and  $k_F^\downarrow = \sqrt{2m(E_F - \Delta/2)}/\hbar$ .

The transport through an interface between such a magnetic metal and the nanotube is determined by the overlap between the corresponding Fermi surfaces. Three scenarios are possible. First the Fermi-wave vector of the carbon nanotube is smaller than both  $k_F^\uparrow$  and  $k_F^\downarrow$  (see fig-

ure 18a). In this case in the magnetic metal there is always a  $k$ -vector that matches the Fermi-wave vector of the nanotube for both spins. Therefore both spins can be injected into the tube and the total resistance will be small and spin-independent.

Secondly the Fermi-wave vector of the carbon nanotube is larger than both  $k_F^\uparrow$  and  $k_F^\downarrow$  (see figure 18b). Now no states are available in the metallic contacts whose wave-vectors match the Fermi wave-vector of the carbon nanotube. For zero-bias and zero-temperature the resistance is extremely large. Nevertheless upon increasing the temperature, phonon assisted transport becomes possible. Spin electrons can be scattered out of the Fermi surface into states with large longitudinal momentum. At temperature  $T$  the fraction of electrons with energy above  $E_F$  is simply proportional to the Fermi distribution function. However, because of the exchange energy, spin-up electrons will possess higher momentum than spin-down. Therefore one can find more spin-up states with a longitudinal momentum matching the one of the nanotube than spin-down states. This potentially gives a temperature-induced spin-dependent resistance.

Finally if the Fermi wave-vector of the carbon nanotube is larger than  $k_F^\downarrow$  but smaller than  $k_F^\uparrow$  (see figure 18c), only the majority electrons can enter the nanotube. The system becomes fully spin-polarized and the Fermi surface matching replaces the bonding spin-selectivity encountered in the previous section. Also in this case a spin-valve structure made by magnetic contacts and carbon nanotube as spacer is predicted to show infinite GMR at zero temperature. An increase of the temperature will produce a degradation of the polarization since minority spins can be thermally scattered outside their Fermi surface, and therefore contribute to the transport.

Two important aspects must be pointed out. First all these considerations are based on the assumption of perfectly crystalline systems. This may not be true in reality and the effects of breaking the translational invariance must be considered. From a qualitative point of view disorder smears the Fermi surface and eventually may produce some states with large longitudinal momentum. This will improve the conductance through the nanotube, even if its spin-polarization will be in general dependent on the nature of disorder.

Secondly, our heuristic argument does not necessarily apply to the case of transition metal contacts, where the spin-selectivity arising from the different bonding nature of the two spin-subbands can play an important rôle. Clearly more realistic bandstructure calculations are needed. These however are rather problematic. In addition to the need of simulating transition metal leads one has to consider rather large supercell for a reasonable description of the nanotube/metal interface.

For this reason most of the calculations to date have used simple tight-binding models without self-consistent procedures<sup>88,89,90</sup>. These roughly agree on the possibility of large GMR ratios in transition metals contacted nanotubes, although the actual values predicted are some-

how affected by the different methods and the contact geometry.

### C. Long molecules and phonons

As mentioned previously electronic transport in polymers and long molecules offer a considerable higher level of complexity when compared to small ballistic molecules. The first consideration is that the transport is often driven by strong electron-phonon interaction, therefore the relevant current carriers are some correlated electronic-vibronic states (polarons, bi-polarons, etc.). Moreover in the case of spin-transport one has to take into account the likely presence of paramagnetic centers<sup>60</sup>. They usually appear in low concentrations, but they become relevant to the spin-dynamics in long molecules. These two features add to the large scale of the system and make the problem of spin-transport in large organic molecules intractable with *ab initio* methods. This is the main reason why to date only simple Hamiltonian models have been used.

When the electron-phonon interaction is weak, or alternatively the molecule is rather short in such a way that polaronic-type of transport is not dominant, then phonon absorption/emission has only the effect of smearing the transmission coefficient. In spin-valves made from transition metals such a smearing is likely to result in a reduction of the spin-polarization of the device and therefore of the GMR<sup>91</sup>. However quantitative predictions are difficult, since also in this case a detailed description of the electronic structure of the electrodes and of the bonding with the molecule is essential. For instance calculations of spin-injection into short strands of DNA obtained with simple single-orbital tight-binding models and some parameterization of the metal/molecule bonding, report both an enhancement<sup>92</sup> and a reduction<sup>93</sup> of the GMR with the bias.

When the electron-phonon interaction is strong and the molecules are rather long, then the ground state of the molecule is some correlated electronic-vibronic state. In this case the situation is more complex and to the best of our knowledge no transport calculations have been carried out to date. Some interesting insights come from the investigation of the ground state of polymers in contact with magnetic metals. Xie and co-workers<sup>61</sup> investigated a non-degenerate polymer in contact with a model metal reproducing either a magnetic transition metal or manganese. Interestingly they found that when no charge is transferred from the metal to the polymer, this remains metallic with a rather uniform distribution of the charge across the interface. In contrast charge transfer promotes the formation of spinless bipolarons in the polymers. An analysis of the DOS of the whole structure further suggest that the bipolaron formation drastically reduces the spin polarization of the whole system.

## VI. MORE EXOTIC PHENOMENA

### A. Molecular Magnets

Extremely interesting features appear in quantum transport through molecules when the conducting electrons interact with some internal molecular degrees of freedom. This is for instance the case of vibrational levels, where electron-phonon interaction manifests itself with sharp changes in the slope of the  $I$ - $V$  curve, steps in  $dI/dV$  and in peaks in  $d^2I/dV^2$ . It is therefore natural to speculate about similar effects associated to internal magnetic degrees of freedom, i.e. the molecular spin<sup>94</sup>. Until recently the experimental activity was focussed on reproducing at the molecular level effects already demonstrated in quantum dots, such as the Zeeman splitting of the Coulomb-blockade as well as the Kondo effect<sup>95,96</sup>. More recently, advances in the chemical functionalization of magnetic molecules have allowed the formation of stable bonding between the molecules and metallic surfaces<sup>97,98</sup>, thus the construction of two and three terminal devices<sup>99,100</sup>.

Magnetic molecules<sup>101</sup> are molecules comprising a number of transition metal ions magnetically coupled to each other in such a way to give rise to a global net spin  $S$ . They are usually described by the following spin Hamiltonian  $H_0$

$$H_0 = DS_z^2 + g\mu_B H_z S_z, \quad (13)$$

where  $D$  ( $D < 0$ ) is the zero field splitting constant and  $H_z$  is the  $z$  component of an external magnetic field ( $\mu_B$  is the Bohr magneton). The term proportional to  $S_z^2$  lift the degeneracy of the spin-multiplet and the energy levels can be labeled by the magnetic quantum number  $M_S$ , with  $-S \leq M_S \leq S$ .

If the dynamics is solely determined by the Hamiltonian  $H_0$  then a molecule prepared in a given  $M_S$  state will remain in such state. However a perturbation  $H_1$ , which does not commute with  $H_0$  will create mixing between the  $M_S$  states, thus transition between levels with different  $M_S$  will be possible. Selection rules for these transitions are given by the particular symmetry of the perturbation, and for instance transverse anisotropy

$$H_1 = E(S_x^2 - S_y^2), \quad (14)$$

allows transitions  $M_S \rightarrow M_S \pm 2n$  with  $n$  an integer. Evidence of quantum tunneling of the magnetization for magnetic molecules are now numerous<sup>101</sup>.

Let us now consider the case of electronic transport through such a molecule and in particular the case of weak coupling between the molecule and the current/voltage electrodes, which is the most likely situation in actual experiments<sup>99,100</sup>. In general the ground state for a charged molecule will be different from that of its neutral state, and so will be the excitation spectrum. This means that sequential tunneling can potentially leave the molecule in some excited state not allowed

to relax by the selection rules. Importantly also the opposite is true, namely that a charged excited molecule can relax to a state which does not allow electron transfer to the electrodes because of the selection rules. This may lead to a complete suppression of the current<sup>99</sup>.

Two experimental works have been published so far on transport through magnetic molecules<sup>99,100</sup>. They both consist in a transistor geometry where a single  $Mn_{12}$  molecule is trapped.  $Mn_{12}$ ,  $[Mn_{12}O_{12}(CH_3COO)_{16}(H_2O)_4]$ , is perhaps the prototype of all molecular magnets. The 12 Mn ions occupy three inequivalent atomic sites, namely two  $Mn^{3+}$  and one  $Mn^{4+}$ . The Mn ions with different valence couple antiferromagnetically to each other resulting in a total  $S = 10$  ground state. In one case the molecule has been functionalized (see figure 19) with thiol groups in order to form stable contacts with the gold surfaces of the electrodes. The crucial aspect of both these experiments is the discovery of fingerprints of the molecular state into the  $I$ - $V$  characteristics of the device. In particular negative differential conductance, complete current suppression<sup>99</sup> and non-trivial dependence of the peaks in the differential conductance over an applied magnetic field<sup>100</sup>, can all be interpreted as a result of the internal spin-dynamics of the molecule.

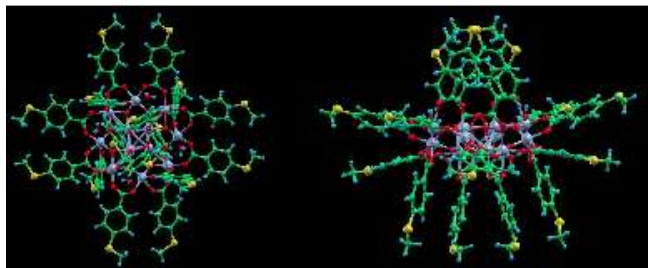


Figure 19: Top and side views of a ball-and-stick model for a  $Mn_{12}$  magnetic molecule. In this case we consider  $[Mn_{12}O_{12}(O_2C-R-SAc)_{16}(H_2O)_4]$  where  $R = \{C_6H_4, C_{15}H_{30}\}$ . Colour code: green=carbon, yellow=sulphur, blue=hydrogen, red=oxygen and violet=manganese.

Several model calculations have been performed for explaining the various features of these experiments<sup>102</sup> and proposing a new setup where one of the electrodes is a ferromagnet<sup>103,104</sup>. These are based on the spin-Hamiltonian of equations (13) and (14) and an additional term that takes into account the coupling with the electrodes. Then the transport calculation is performed within the standard master equation formalism familiar to transport through interacting quantum dots<sup>105</sup>. Although these calculations are certainly important since they demonstrate the mechanisms behind the various effects, they depend heavily on the specific choice of the parameters used. For this reason *ab initio* simulations would be very important. For instance questions about the actual charging state of the molecule under bias, the strength of the interaction between the conducting elec-

trons and the Mn ions, and the electrical response of the whole system are likely to find an answer with DFT calculations. The problem is indeed complicated and even the simple evaluation of the ground state of magnetic molecules from DFT is not trivial<sup>106,107</sup>. For this reason no first principle calculations of transport through magnetic molecules have been performed to date. However we believe that this is an extremely challenging field where order-N capability, strong correlation and scalable quantum transport schemes can find a common playground.

Finally we want to discuss the possibility of constructing all-molecular spin-valves, i.e. spin-valves where both the spin-injector and spin-detector are molecules or part of the same molecule and the metallic current/voltage electrodes have the only function of electron reservoirs. Also in this case the expectation is to detect electrically the magnetic state of the molecule, however for spin-valve operation we also demand the possibility of switching reversibly between two spin-configurations by applying a magnetic field. An interesting proposal is that of using dicobaltocene molecules<sup>108</sup>. These belong to the metallocene family and are characterized by two Co ions separated by a spacer that can be chemically engineered.

DFT calculations<sup>108</sup> show that dicobaltocene attached to gold electrodes in its ground state is stabilized by superexchange in an antiferromagnetic configuration, i.e. the local moments of the two Co ions are antiparallel to each other. As in a conventional spin-valve a parallel alignment can be obtained by applying a large magnetic field (around 20 T for a C<sub>2</sub>H<sub>4</sub> spacer), and the calculation shows a rather large GMR ratio. This is suggestive of the possibility of all-molecular spin-valves and future experiments in this area are certainly welcome.

## B. d<sup>0</sup> ferromagnetism and magnetic proximity

We wish to close this review with a brief discussion of two recently discovered intriguing phenomena, that challenge our current understanding of ferromagnetism and may offer a new playground for spin-transport. These are d<sup>0</sup> ferromagnetism and magnetic proximity effect. The measurement of long-range ferromagnetic order in materials not containing ions with either *d* or *f* electrons, therefore without an obvious way to produce a local magnetic moment, is the common factor of these two aspects of magnetism.

Let us consider first the case of d<sup>0</sup> ferromagnetism<sup>109</sup>. This is the intrinsic ferromagnetism of usually highly defective materials, which do not contain any partially filled *d* or *f* shells. Among the several examples we wish to mention irradiated graphite and fullerenes<sup>110</sup>, nonstoichiometric CaB<sub>6</sub><sup>111</sup>, and HfO<sub>2</sub> thin films<sup>112</sup>. A common explanation for the magnetism in all these materials is not available at present. Note that one has to explain both the formation of a magnetic moment and the long-range coupling between moments. Generally the moments are associated to intrinsic defects. Paramag-

netic defects in organic materials are not uncommon<sup>60</sup> and strongly correlated molecular orbitals associated to vacancies have been suggested for magnetic oxides<sup>113,114</sup>. However the demonstration of long range coupling remains elusive. For instance recent DFT calculations<sup>115</sup> demonstrate, at least for CaO, that the defect concentration needed for long range ferromagnetism is three orders of magnitude larger than that obtainable at equilibrium. Finally we wish to mention that ferromagnetism originating from *p*-shells has been suggested for oxygen mixed valence compounds such as Rb<sub>4</sub>O<sub>6</sub><sup>116</sup>.

In contrast to d<sup>0</sup> ferromagnetism magnetic proximity is not an intrinsic material property and it does require the presence of a magnetic material. The basic idea is quite simple: there is always some charge transfer at the contact between a conducting molecule and a metal associated with the alignment of their respective chemical potentials. In a ferromagnet some degree of spin transfer accompanies the charge transfer giving rise to an induced magnetic moment. Note that the magnetic proximity effect does not imply intrinsic ferromagnetism and no spin aligning potential exists in the non-magnetic material. This means that a magnetic moment is detected only when a second ferromagnetic material is present and when good contact is made.

A first indirect evidence of this effect was found in explaining the unaccounted magnetization in a carbon meteorite rich of magnetic inclusions<sup>117</sup>. Then Ferreira and Sanvito derived a close system of equations for the induced magnetic moment and for the energetic of a carbon nanotube deposited on a magnetic surface<sup>118</sup>. The calculation, based on a simple tight-binding model, revealed that induced magnetic moments of the order of 0.1 μ<sub>B</sub> per carbon atom in contact can be achieved at room temperature. This paved the way for a more controlled set of experiments.

Experimentally the problem is to detect the small induced moment over a huge background coming from the ferromagnetic substrate. One possible strategy is that of measuring the stray field around the nanotube once this is placed on a smooth thin film. A uniformly magnetized thin film creates no stray field whatever its direction of magnetization. In contrast a magnetized nanotube will produce a stray field, which will be directly detectable. This idea was exploited in the experiments from Céspedes et al.<sup>119</sup>, who measured induced magnetic moments in excess of 0.1 μ<sub>B</sub> per carbon atom in contact, in good agreement with the theoretical prediction. The experiment consists in taking AFM and MFM images of nanotubes on various surfaces. The difference between the topographic (AFM) and the magnetic images (MFM) is a direct measure of the stray field coming from the nanotube and therefore provides evidence for the induced magnetic moment (see figures 20 and 21).

In the another experiment, Mertins et al.<sup>120</sup> produced a multilayer of thin, alternating iron and carbon layers, of thickness 2.55 and 0.55 nm, respectively. Then, they probed locally the magnetic moment of the carbon by X-



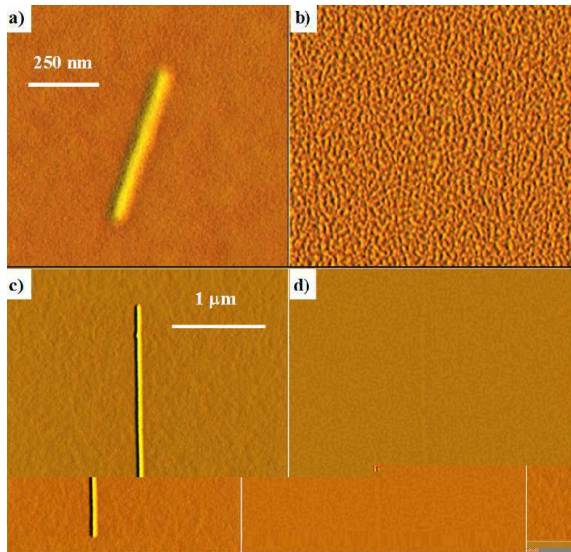


Figure 20: AFM images of a carbon nanotube on copper a) and silicon c) substrate and their corresponding MFM scans b) and d). The MFM images do not show any magnetic contrast indicating no induced magnetic moment.

ray magneto-optical reflectivity of polarized synchrotron radiation. In this type of measurement the Fe and C absorption edges differ by about 500 eV enabling one of establishing with precision whether the magnetic moment comes from C or not. With this method magnetic moments of the order of  $0.05 \mu_B$  were found.

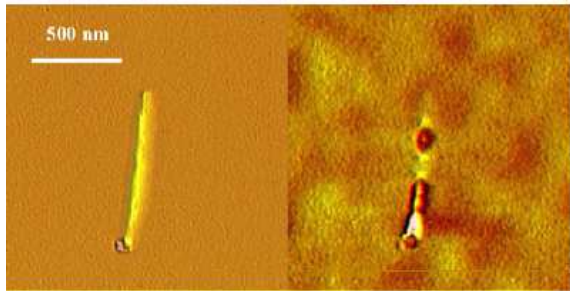


Figure 21: AFM images of a carbon nanotube on cobalt substrate (left) and the corresponding MFM scans (right). The MFM image shows magnetic contrast indicating an induced magnetic moment.

Finally we wish to mention a few experiments where

ferromagnetism is claimed in heterostructures in which none of the components is ferromagnetic. This is for instance the case of gold surfaces and nanoparticles coated with different organic molecules<sup>121,122,123</sup>. Common features to these heterostructures are the extreme magnetic anisotropy and the fact that the magnetization is almost independent from the temperature. A possible explanation is that the charge transfer between the molecule and the substrate and the peculiar 2D properties of the organic layers result in the formation of triplet states with consequent boson condensation<sup>124</sup>. In addition a crucial rôle of spin-orbit interaction has been suggested<sup>125</sup>. To our knowledge, no first principles calculations of these systems have been performed.

## VII. CONCLUSIONS

We have reviewed the most recent advances in spin-transport through organic molecules. This is a new challenging field where disciplines such as physics, chemistry, biology and electronic engineering are rapidly converging. In particular we have discussed the main advantages and perspectives of spin-phenomena at the molecular level.

From a theoretical side *ab initio* methods for quantum transport are rapidly approaching the limit where quantitative predictions of molecular transport can be made. Spin-transport however brings additional complexity since magnetism and strong electron correlation must be considered. These call for even more sophisticated algorithms capable of high accuracy and of undemanding scaling with the system size, an enormous challenge for the future. Finally more and more experiments are appearing where the interaction between conducting electrons and internal molecular degrees of freedom are important. Such systems go way beyond our present computational capabilities in terms of *ab initio* theories and open a completely unexplored way.

## Acknowledgement

We wish to thank Cormac Toher, Ivan Rungger, Chaitanya Das Pemmaraju and Miguel Afonso Oliveira for useful discussions and Hang Guo for giving us access to unpublished material. Figures 20 and 21 are courtesy of J.M.D. Coey and O. Céspedes. This work is sponsored by Science Foundation of Ireland under the grants SFI02/IN1/I175 and SFI05/RFP/PHY0062.

\* Electronic address: sanvitos@tcd.ie

<sup>1</sup> M.N. Baibich, J.M. Broto, A. Fert, F. Nguyen Van Dau, F. Petroff, P. Etienne, G. Creuzet, A. Friederich and J. Chazelas, Phys. Rev. Lett. **61**, 2472 (1988).

<sup>2</sup> G. Binasch, P. Grünberg, F. Saurenbach and W. Zinn,

Phys. Rev. B **39**, 4828 (1989).

<sup>3</sup> S. A. Wolf et al., Science **294**, 1488 (2001).

<sup>4</sup> G. Prinz, Science **282**, 1660 (1998).

<sup>5</sup> G. Prinz, Phys. Today **48**, 58 (1995).

<sup>6</sup> J. M. Kikkawa and D. D. Awschalom, Phys. Rev. Lett.

- 80**, 4313 (1998).
- <sup>7</sup> J. M. Kikkawa and D. D. Awschalom, *Nature* **397**, 139 (1999).
  - <sup>8</sup> D. P. D. Vincenzo, *Science* **270**, 255 (1995).
  - <sup>9</sup> S. Datta and B. Das, *Appl. Phys. Lett.* **56**, 665 (1990)
  - <sup>10</sup> E. I. Rashba, *Sov. Phys. Solid State* **2**, 1109 (1960)
  - <sup>11</sup> Y. K. Kato, R. C. Myers, A. C. Gossard and D. D. Awschalom, *Science Express* **306**, 1910 (2004)
  - <sup>12</sup> M.I. Dyakonov and V.I. Perel, *Sov. Phys. JETP* **38**, 177 (1974).
  - <sup>13</sup> C. Joachim, J. K. Gimzewski, and A. Aviram, *Nature (London)* **408**, 541 (2000).
  - <sup>14</sup> J. Chen, M. A. Reed, A. M. Rawlett, and J. M. Tour, *Science* **286**, 1550 (1999).
  - <sup>15</sup> Z. Yao, H. W. C. Postman, L. Balents, and C. Dekker, *Nature* **402**, 273 (1999).
  - <sup>16</sup> P.J. Kuekes, J.R. Heath, and R.S. Williams, US Patent, number 6128214 (Hewlett-Packard), October 2000.
  - <sup>17</sup> S. J. Tans, A. R. M. Verschueren, and C. Dekker, *Nature* **393**, 49 (1998).
  - <sup>18</sup> C.P. Collier, E.W. Wong, M. Belohradsky, F.M. Raymo, J.F. Stoddart, P.J. Kuekes, R.S. Williams and J.R. Heath, *Science* **285**, 391 (1999).
  - <sup>19</sup> Y. Huang, X. Duan, Y. Cui, L.J. Lauhon, K.-H. Kim, C.M. Lieber, *Science* **294**, 1313 (2001).
  - <sup>20</sup> K. Tsukagoshi, B. W. Alphenaar, and H. Ago, *Nature (London)* **401**, 572-574 (1999).
  - <sup>21</sup> J. R. Petta, S. K. Slater and D. C. Ralph, *Phys. Rev. Lett.* **93**, 136601 (2004).
  - <sup>22</sup> Z. H. Xiong, D. Wu, Z. Valy Vardeny and J. Shi, *Nature (London)* **427**, 821-824 (2004).
  - <sup>23</sup> V. Dediu, M. Murgia, F.C. Matocotta, C. Taliani, and S. Barbanera, *Solid State Commun.* **122**, 181-184 (2002).
  - <sup>24</sup> M. Ouyang and D. D. Awschalom, *Science* **301**, 1074-1078 (2003).
  - <sup>25</sup> C.K. Chiang, C.R. Fincher, Jr., Y.W. Park, A.J. Heeger, H. Shirakawa, E.J. Louis, S.C. Gau, and A.G. MacDiarmid, *Phys. Rev. Lett.* **39**, 1098 (1977).
  - <sup>26</sup> D. Gatteschi, R. Sessoli and J. Villain, *Molecular Nanomagnets*, Oxford University Press (Oxford, 2006)
  - <sup>27</sup> A.R. Rocha, V.M. García-Suárez, S.W. Bailey, C.J. Lambert, J. Ferrer and S. Sanvito, *Phys. Rev. B* **73**, 085414 (2006); see also [www.smeagol.tcd.ie](http://www.smeagol.tcd.ie)
  - <sup>28</sup> A.R. Rocha, V.M. García-Suárez, S.W. Bailey, C.J. Lambert, J. Ferrer and S. Sanvito, *Nature Materials* **4**, 335 (2005).
  - <sup>29</sup> J. Taylor, H. Guo, and J. Wang, *Phys. Rev. B* **63**, 245407 (2001).
  - <sup>30</sup> Y. Xue, S. Datta and M.A. Ratner, *Chem. Phys.* **281**, 151 (2002).
  - <sup>31</sup> M. Bradbyge, J. Taylor, K. Stokbro, J.-L. Mozos, and P. Ordejón, *Phys. Rev. B* **65**, 165401 (2002).
  - <sup>32</sup> J. J. Palacios, A. J. Pérez-Jiménez, E. Louis, E. SanFabián, and J. A. Vergés, *Phys. Rev. B* **66**, 035322 (2002).
  - <sup>33</sup> A. Pecchia and A. Di Carlo, *Rep. Prog. Phys.* **67**, 1497 (2004).
  - <sup>34</sup> H. Hohenberg and W. Kohn, *Phys. Rev.* **136**, B864 (1964).
  - <sup>35</sup> C. Toher, A. Filippetti, S. Sanvito and K. Burke, *Phys. Rev. Lett.* **95** 146402 (2005).
  - <sup>36</sup> M. Stamenova, S. Sanvito and T. Todorov, *Phys. Rev. B* **72**, 134407 (2005).
  - <sup>37</sup> J.M.D. Coey and S. Sanvito, *Physics World*, November pag. 33, (2004)
  - <sup>38</sup> J. M. Soler, E. Artacho, J. D. Gale, A. García, J. Junquera, P. Ordejón and D. Sanchez-Portal, *J. Phys. Cond. Matter* **14**, 2745-2779 (2002).
  - <sup>39</sup> T.-S. Choy, Ph.D. Thesis, University of Florida (2001), <http://www.phys.ufl.edu/fermisurface/>.
  - <sup>40</sup> J.C. Slater, *J. Appl. Phys.* **8**, 385 (1937)
  - <sup>41</sup> L. Pauling, *Phys. Rev.* **54**, 899 (1938)
  - <sup>42</sup> J.M.D. Coey and S. Sanvito, *J. Phys.: Appl. Phys.* **37**, 988 (2004).
  - <sup>43</sup> N. Mott, *Proc. Roy. Soc. A* **153**, 699 (1936).
  - <sup>44</sup> I. I. Mazin, *Phys. Rev. Lett.* **83**, 1427 (1999).
  - <sup>45</sup> S. P. Lewis, P. B. Allen, and T. Sasaki, *Phys. Rev. B* **55**, 10253 (1997).
  - <sup>46</sup> B. Nadgorny et al., *Phys. Rev. B* **63**, 184433 (2001).
  - <sup>47</sup> D. Singh, *Phys. Rev. B* **55**, 313 (1997).
  - <sup>48</sup> J. de Teresa et al., *Science* **286**, 507 (1999).
  - <sup>49</sup> S. Datta, *Nanotechnology* **15**, S433 (2004).
  - <sup>50</sup> B. C. Stipe, M. A. Rezaei, and W. Ho, *Science* **280**, 1732 (1998).
  - <sup>51</sup> A. P. Sutton, *Electronic Structure of Materials*, Oxford University Press, Oxford, UK, 1996.
  - <sup>52</sup> P.S. Krastic, D.J. Dean, X.-G. Zhang, D. Keffer, Y.S. Leng, P.T. Cummings, and J.C. Wells, *Comp. Mat. Sci.* **28**, 321 (2003)
  - <sup>53</sup> J.H. Davies, *The Physics of Low-dimensional Semiconductors : An Introduction*, Cambridge University Press (December 13, 1997)
  - <sup>54</sup> J. Serrano, M. Cardona and T. Ruf, *Solid State Commun.* **113**, 411 (2000)
  - <sup>55</sup> A. Khaetskii, D. Loss and L. Glazman, *Phys. Rev. B* **67**, 195329 (2003)
  - <sup>56</sup> G. Salis, D.T. Fuchs, J.M. Kikkawa, D.D. Awschalom, Y. Ohno and H. Ohno, *Phys. Rev. Lett.* **86**, 2677 (2001).
  - <sup>57</sup> M. Julliere, *Phys. Lett. A* **50**, 225 (1975).
  - <sup>58</sup> S. Pramanik, C-G. Stefanita, S. Bandyopadhyay, N. Harth, K. Garre, M. Cahay, *cond-mat/0508744*
  - <sup>59</sup> A.J. Heeger, S. Kivelson, J.R. Schrieffer and W.P. Su, *Rev. Mod. Phys.* **60**, 782 (1988).
  - <sup>60</sup> V.I. Krinichnyi, *Synth. Metals*, **108**, 173 (2000)
  - <sup>61</sup> S.J. Xie, K.H. Ahn, D.L. Smith, A.R. Bishop, and A. Saxena, *Phys. Rev. B* **67** 125202 (2003)
  - <sup>62</sup> M. Koentopp, K. Burke and F. Evers, *Phys. Rev. B* **73**, 121403(R) (2006).
  - <sup>63</sup> H. Haug and A. P. Jauho, *Quantum Kinetics in Transport and Optics of Semiconductors*, Springer, Berlin, 1996.
  - <sup>64</sup> S. Sanvito, C. J. Lambert, J. H. Jefferson, and A.M. Bratkovsky, *Phys. Rev. B* **59**, 11936-11948 (1999).
  - <sup>65</sup> E. G. Emberly and G. Kirczenow, *Chem. Phys.* **281**, 311-324 (2002).
  - <sup>66</sup> R. Pati, L. Senapati, P.M. Ajayan, and S.K. Nayak, *Phys. Rev. B* **68**, 100407(R) (2003).
  - <sup>67</sup> R. Pati, M. Mailman, L. Senapati, P.M. Ajayan, S.D. Mahanti and S.K. Nayak, *Phys. Rev. B* **68**, 014412 (2003)
  - <sup>68</sup> L. Senapati, R. Pati, M. Mailman and S.K. Nayak, *cond-mat/0408462*
  - <sup>69</sup> Y. Wei, Y. Xu, J. Wang and H. Guo, *Phys. Rev. B* **70**, 193406 (2004).
  - <sup>70</sup> Note that this is the DFT-LDA gap, which might be substantially smaller than the actual gap.
  - <sup>71</sup> J. Tomfohr and O. Sankey, *Phys. Rev. B* **65**, 245105 (2002).
  - <sup>72</sup> C. Tiusan, J. Faure-Vincent, C. Bellouard, M. Hehn, E. Jouguelet and A. Schuhl, *Phys. Rev. Lett.* **93** 106602 (2004).

- <sup>73</sup> K. D. Belashchenko, J. Velev, and E. Y. Tsymbal, *Phys. Rev. B* **72**, 140404(R) (2005).
- <sup>74</sup> H. Dalglish and G. Kirczenow, *Phys. Rev. B* **72**, 184407 (2005).
- <sup>75</sup> D. Waldron, P. Haney, B. Larade, A. MacDonald and H. Guo, *Phys. Rev. Lett.* **96**, 166804 (2006).
- <sup>76</sup> R. Saito, G. Dresslhaus, and M. Dresselhaus, *Physical Properties of Carbon Nanotubes*, Imperial College Press, London, 1996.
- <sup>77</sup> S. Franck, P. Poncharal, Z. Wang, and W. de Heer, *Science* **280**, 1744 (1998).
- <sup>78</sup> C. White and T. Todorov, *Nature* **393**, 240 (1998).
- <sup>79</sup> B. Zhao, I. Mönch, T. Mühl, H. Vinzelberg, and C. Schneider, *J. Appl. Phys.* **91**, 7026 (2002).
- <sup>80</sup> B. Zhao, I. Mönch, H. Vinzelberg, T. Mühl, and C. Schneider, *Appl. Phys. Lett.* **80**, 3144 (2002).
- <sup>81</sup> S. Sahoo, T. Kontos, C. Schönenberger, and C. Sürgers, *Appl. Phys. Lett.* **86**, 112109 (2005).
- <sup>82</sup> A. Jensen, J. Nygard, and J. Borggreen, in *Toward the controllable quantum states*, Proceedings of the International Symposium on Mesoscopic Superconductivity and Spintronics, H. Takayanagi and J. Nitta, 33 (2003).
- <sup>83</sup> S. Sahoo, T. Kontos, J. Furer, C. Hoffmann, M. Gräber, A. Cottet and C. Schönenberger, *Nature Physics* **1**, 99 (2005).
- <sup>84</sup> B. Nagabhirava, T. Bansal, G. U. Sumanasekera, and B. W. Alphenaar, *Appl. Phys. Lett.* **88**, 023503 (2006).
- <sup>85</sup> L.E. Hueso, J.M. Pruneda, V. Ferrari, G. Burnell, J.P. Valdes-Herrera, B.D. Simons, P.B. Littlewood, E. Artacho, and N.D. Mathur, *cond-mat/0511697*.
- <sup>86</sup> J. Tersoff, *Appl. Phys. Lett.* **74**, 2122 (1999).
- <sup>87</sup> P. Delaney and M. D. Ventra, *Appl. Phys. Lett.* **75**, 4028 (1999).
- <sup>88</sup> H. Mehrez, J. Taylor, H. Guo, J. Wang, and C. Roland, *Phys. Rev. Lett.* **84**, 2682 (2000).
- <sup>89</sup> S. Krompiewski, R. Gutierrez, and G. Cuniberti, *Phys. Rev. B* **69**, 155423 (2004).
- <sup>90</sup> S. Krompiewski, *J. Phys.: Condens. Matter* **16**, 2981 (2004).
- <sup>91</sup> N. Jean and S. Sanvito, *Phys. Rev. B* (2006).
- <sup>92</sup> M. Zwolak and M. Di Ventra, *Appl. Phys. Lett.* **81**, 925 (2002)
- <sup>93</sup> X.F. Wang and T. Chakraborty, *cond-mat/0512473*
- <sup>94</sup> G.-H. Kim and T.-S. Kim, *Phys. Rev. Lett.* **92**, 137203 (2004).
- <sup>95</sup> J. Park, A.N. Pasupathy, J.I. Goldsmith, C. Chang, Y. Yaish, J.R. Petta, M. Rinkoski, J.P. Sethna, H.D. Abruna, P.L. McEuen, and D.C. Ralph, *Nature (London)* **417**, 722 (2002).
- <sup>96</sup> W. Liang, M.P. Shores, M. Bockrath, J.R. Long and H. Park, *Nature (London)* **417**, 725 (2002).
- <sup>97</sup> A. Cornia, A.C. Fabretti, M. Pacchioni, L. Zoppi, D. Bonacchi, A. Caneschi, D. Gatteschi, R. Biagi, U. del Pennino, V. De Renzi, I.Gurevish and H.J. van der Zant, *Angew. Chem. Int. Ed.* **42**, 1645 (2003).
- <sup>98</sup> M. Mannini, D. Bonacchi, L. Zoppi, F.M. Piras, E.A. Speets, A. Caneschi, A. Cornia, A. Magnani, B.J. Ravoo, D.N. Reinhoudt, R. Sessoli and D. Gatteschi, *Nano Lett.* **5**, 1435 (2005).
- <sup>99</sup> H.B. Heersche, Z. de Groot, J.A. Folk, H.S.J. van der Zant, C. Romeike, M.R. Wegewijs, L. Zoppi, D. Barreca, E. Tondello and A. Cornia, *cond-mat/0510732*.
- <sup>100</sup> M.-H. Jo, J.E. Grose, K. Baheti, M.M. Deshmukh, J.J. Sokol, E.M. Rumberger, D.N. Hendrickson, J.R. Long, H. Park and D.C. Ralph, *cond-mat/0603276*.
- <sup>101</sup> D. Gatteschi and R. Sessoli, *Angew. Chem. Int. Ed.* **42**, 1268 (2003).
- <sup>102</sup> C. Romeike, M.R. Wegewijs and H. Schoeller, *cond-mat/0511391*.
- <sup>103</sup> F. Else and C. Timm, *cond-mat/0601294*.
- <sup>104</sup> F. Else and C. Timm, *cond-mat/0511291*.
- <sup>105</sup> A. Thielmann, M.H. Hettler, J. König and G. Schön, *Phys. Rev. B* **68**, 115105 (2003).
- <sup>106</sup> K. Park, M.R. Pederson and C.S. Hellberg, *Phys. Rev. B* **69**, 014416 (2004).
- <sup>107</sup> K. Park and M.R. Pederson, *Phys. Rev. B* **70**, 054414 (2004).
- <sup>108</sup> R. Liu, S.-H. Ke, H.U. Baranger and W. Yang, *Nano Lett.* **5**, 1959 (2005).
- <sup>109</sup> J.M.D. Coey, *Solid State Sciences* **7**, 660667 (2005).
- <sup>110</sup> T.L. Makarova, *Semiconductors* **38**, 615 (2004).
- <sup>111</sup> D.P. Young, D. Hall, M.E. Torelli, Z. Fisk, J.L. Sarrao, J.D. Thompson, H.R. Ott, S.B. Oseroff, R.G. Goodrich, R. Zysler, *Nature (London)* **397**, 412 (1999).
- <sup>112</sup> M. Venkatesan, C.B. Fitzgerald, J.M.D. Coey, *Nature (London)* **430**, 630 (2004).
- <sup>113</sup> Chaitanya Das Pemmaraju and S. Sanvito, *Phys. Rev. Lett.* **94**, 217205 (2005).
- <sup>114</sup> I.S. Elfimov, S. Yunoki and G.A. Sawatzky, *Phys. Rev. Lett.* **89**, 216403 (2002).
- <sup>115</sup> J. Osorio-Guillén, S. Lany, S.V. Barabash and A. Zunger, *Phys. Rev. Lett.* **96**, 107203 (2006).
- <sup>116</sup> J.J. Attema, G.A. de Wijs, G.R. Blake and R.A. de Groot, *J. Am. Chem. Soc.* **127**, 16325 (2005).
- <sup>117</sup> J. Coey, M. Venkatesan, C. Fitzgerald, A. Douvalis, and I. Sanders, *Nature* **420**, 156 (2002).
- <sup>118</sup> M. Ferreira and S. Sanvito, *Phys. Rev. B* **69**, 035407 (2004).
- <sup>119</sup> O. Céspedes, M. S. Ferreira, S. Sanvito, M. Kociak, and J. M. D. Coey, *J.Phys.: Condens Matter* **16**, L155 (2004).
- <sup>120</sup> H. Mertins et al., *Europhys. Lett.* **66**, 743 (2004).
- <sup>121</sup> S.G. Ray, S.S. Daube, G. Leitus, Z. Vager and R. Naaman, *Phys. Rev. Lett.* **96**, 036101 (2006)
- <sup>122</sup> P. Crespo, R. Litrán, T.C. Rojas, M. Multigner, J.M. de la Fuente, J.C. Sánchez-López, M.A. Garca, A. Hernando, S. Penadés and A. Fernández, *Phys. Rev. Lett.* **93**, 087204 (2004).
- <sup>123</sup> Y. Yamamoto, T. Miura, M. Suzuki, N. Kawamura, H. Miyagawa, T. Nakamura, K. Kobayashi, T. Teranishi and H. Hori, *Phys. Rev. Lett.* **93**, 116801 (2004).
- <sup>124</sup> Z. Varg and R. Naaman, *Phys. Rev. Lett.* **92**, 087205 (2004).
- <sup>125</sup> A. Hernando, P. Crespo and M.A. Garcia, *Phys. Rev. Lett.* **96**, 057206 (2006).